⌘ Author's Choice

Glycoproteomic Analysis of the Secretome of Human Endothelial Cells*[S]

Xiaoke Yin‡, Marshall Bern§, Qiuru Xing‡, Jenny Ho¶, Rosa Viner‖, and Manuel Mayr‡**

Previous proteomics studies have partially unraveled the complexity of endothelial protein secretion but have not investigated glycosylation, a key modification of secreted and membrane proteins for cell communication. In this study, human umbilical vein endothelial cells were kept in serum-free medium before activation by phorbol-12-myristate-13 acetate, a commonly used secretagogue that induces exocytosis of endothelial vesicles. In addition to 123 secreted proteins, the secretome was particularly rich in membrane proteins. Glycopeptides were enriched by zwitterionic hydrophilic interaction liquid chromatography resins and were either treated with PNGase F and $H_2{}^{18}O$ or directly analyzed using a recently developed workflow combining higher-energy C-trap dissociation (HCD) with electron-transfer dissociation (ETD) for a hybrid linear ion trap–orbitrap mass spectrometer. After deglycosylation with PNGase F in the presence of $H_2{}^{18}O$, 123 unique peptides displayed ^{18}O-deamidation of asparagine, corresponding to 86 proteins with a total of 121 glycosylation sites. Direct glycopeptide analysis via HCD-ETD identified 131 glycopeptides from 59 proteins and 118 glycosylation sites, of which 41 were known, 51 were predicted, and 26 were novel. Two methods were compared: alternating HCD-ETD and HCD-product-dependent ETD. The former detected predominantly high-intensity, multiply charged glycopeptides, whereas the latter preferentially selected precursors with complex/hybrid glycans for fragmentation. Validation was performed by means of glycoprotein enrichment and analysis of the input, the flow-through, and the bound fraction. This study represents the most comprehensive characterization of endothelial protein secretion to date and demonstrates the potential of new HCD-ETD workflows for determining the glycosylation status of complex biological samples. ***Molecular & Cellular Proteomics 12: 10.1074/mcp.M112.024018, 956–978, 2013.***

Cardiovascular disease manifests predominantly as myocardial ischemia, heart failure, stroke, aortic aneurysm, and peripheral vascular disease and leads to the majority of deaths and disabilities worldwide. Endothelial cells (ECs) constitute the inner lining of all blood vessels and form the interface between the circulation and the vascular wall (1). The endothelial monolayer is pivotal for maintaining vascular homeostasis through a balance of endothelium-derived factors (2, 3). ECs are preferred targets of cardiovascular risk factors such as hypercholesterolemia, diabetes, hypertension, and smoking (1, 4). Repetitive injury is associated with a varying degree of endothelial dysfunction. Alterations in its anticoagulant and anti-inflammatory properties leave the vasculature susceptible to disease (5) and play a key role in the initiation and progression of cardiovascular disease (6).

Previous proteomics studies (7–13), including one by our group (8), have investigated the secretome of unstimulated human umbilical vein ECs (HUVECs), the most widely used ECs in cardiovascular research. Only two studies have explored the secretome of HUVECs upon activation by shear stress (10) or with statin treatment (13) thus far. One study used human microvascular ECs (9), which represent a distinct population of ECs from small vessels. Yet many factors secreted by ECs were not identified, probably because of their low abundance. In this study, we used a secretagogue, phorbol ester phorbol-12-myristate-13-acetate (PMA) (14, 15), to induce maximal protein release from serum-starved HUVECs over 45 min. In addition, we applied three different proteomic strategies for the analysis of glycoproteins/glycopeptides to further enrich secreted proteins and characterize their glycosylation sites.

EXPERIMENTAL PROCEDURES

EC Culture—HUVECs (Lonza Group Ltd., Basel, Switzerland) were cultured on 0.1% gelatin-coated flasks in M199 medium supplemented with 1 ng/ml endothelial cell growth factor (Sigma), 3 μg/ml endothelial growth supplement from bovine neural tissue (Sigma), 10 U/ml heparin, 1.25 μg/ml thymidine, 10% fetal bovine serum (A15–108, PAA Laboratories, Velizy-Villacoublay, France), and 100 μg/ml penicillin and streptomycin in a humidified incubator supplemented with 5% CO_2 at 37 °C. The cells were subcultured every 2 to 3 days at a ratio of 1:4 (16).

Conditioned Medium Collection—HUVECs were cultured in complete medium until confluent. Then, they were washed and incubated in M199 medium for 30 min twice before stimulation with 50 nM PMA (Sigma) in M199 medium for 45 min. The control group was incubated with M199 medium in the absence of PMA for 45 min. Conditioned media were collected and stored at −80 °C for further analysis.

Immunofluorescence Staining—HUVECs were cultured in Nunc chamber slides (Sigma-Aldrich) for 3 days. HUVECs were stimulated

From ‡The King's British Heart Foundation Centre, King's College London, London SE5 9NU, UK; §Protein Metrics, San Carlos, CA 94070; ¶Thermo Fisher Scientific, Hemel Hempstead, HP2 7GE, UK; ‖Thermo Fisher Scientific, San Jose, CA 95134

⌘ *Author's Choice*—Final version full access.

Received September 12, 2012, and in revised form, January 18, 2013

Published, MCP Papers in Press, January 23, 2013, DOI 10.1074/mcp.M112.024018

with 50 nM PMA in M199 medium for 45 min or incubated with M199 medium for 45 min. The cells were fixed with 4% formaldehyde in PBS for 10 min, permeabilized with 0.1% Triton X-100 in PBS for 5 min, and blocked in 5% fetal bovine serum in PBS for 30 min at 37 °C. Following 1 h of incubation with the primary antibodies, VE-cadherin (ab33168, Abcam, Cambridge, UK), and von Willebrand factor (vWF) (sc-8068, Santa Cruz Biotechnology, Santa Cruz, CA) at 37 °C, an Alexa Fluor® 594 conjugated donkey anti-rabbit IgG and an Alexa Fluor® 488 conjugated donkey anti-goat IgG, respectively, were added, and the cells were incubated at 37 °C for 30 min. Nuclei were counterstained with 4′,6-diamidino-2-phenylindole (D9542, Sigma) for 5 min. The slide was mounted in fluorescence mounting medium (DAKO, Denmark A/S, Glostrup, Denmark) and examined with an AxioPlan 2 fluorescence microscope (Carl Zeiss, Thornwood, NY) (17).

Proteomics Profiling of the Secretome—Conditioned media were concentrated with an Amicon spin column (3kD MWCO, EDO Millipore Corp., Billerica, MA) and separated via 4%–12% Bis-Tris SDS-PAGE (Invitrogen). Proteins were visualized via silver staining (PlusOne silver staining kit for proteins, GE Healthcare). Gel bands were digested with modified trypsin (Promega Corp., Madison, WI) overnight on a ProGest digestion robot (Digilab Inc., Marlborough, MA) and analyzed via reverse-phase nano-flow HPLC (PepMap C18, 3 μm, 100 Å, 25 cm $\times$ 75 μm inner diameter column, Thermo Scientific) interfaced to an LTQ Orbitrap XL MS (Thermo Scientific) (18).

Deglycosylation—Concentrated media were mixed with deglycosylation buffer (150 mM NaCl, 50 mM sodium acetate, 10 mM EDTA, proteinase inhibitors, pH 6.8) supplemented with 0.05U PNGase F (Sigma), chondroitinase ABC (C3667, Sigma), and keratanase (G6920, Sigma) and incubated at 37 °C overnight (19).

Immunoblotting—Concentrated or deglycosylated media were separated via 4%–12% Bis-Tris gel (Invitrogen). Proteins were transferred on a nitrocellulose membrane and blocked with 5% bovine serum albumin in PBS. Membranes were incubated with primary antibody overnight at 4 °C. Secondary antibodies were incubated for 1 h at room temperature. After the addition of ECL (GE Healthcare), the film was developed using a Compact X4 Automatic Processor (Xograph Healthcare Ltd., Stonehouse, UK). The following primary antibodies were used: agrin (sc-25528, Santa Cruz Biotechnology), biglycan (ab54855, Abcam), connective tissue growth factor (sc-25440, Santa Cruz Biotechnology), fibronectin (sc-56391, Santa Cruz Biotechnology), and lymphatic vessel endothelial hyaluronic acid receptor 1 (AF2089, R&D Systems).

Difference Gel Electrophoresis—Conditioned media from HUVECs treated with or without PMA were concentrated using an Amicon spin column (3kD MWCO, Millipore) and the ReadyPrep 2D clean-up kit (Bio-Rad). The pellet was resuspended in difference gel electrophoresis lysis buffer (30 mM Tris, 8 M urea, 4% w/v CHAPS, protease inhibitors, pH 8.5). For each secretome sample, 15 μg of proteins were labeled with Cy3 or Cy5. A dye swap was performed to exclude preferential labeling. Cellular extracts of HUVECs were labeled with Cy2. Cy2-, Cy3-, and Cy5-labeled samples were separated via isoelectric focusing on immobilized pH gradient dry strips (18 cm, pH 3–10 NL, GE Healthcare) with 30 KVH. The strips were equilibrated with 10 mg/ml DTT in equilibration buffer (6 M urea, 2% w/v SDS, 30% v/v glycerol, 50 mM Tris, pH 8.8) for 15 min followed by 48 mg/ml iodoacetamide in equilibration buffer for 15 min before separation via SDS-PAGE at 100 W for 4 h using an Ettan DALTsix vertical electrophoresis system (GE Healthcare) (20–22). Gels were scanned on an Ettan difference gel electrophoresis imager (GE Healthcare). Images were overlaid with ImageQuant TL software (GE Healthcare). Common spots present in both the cellular proteome and the secretome were excised, digested with trypsin, and identified using nano-flow HPLC-MS/MS. Detailed protocols are available on our research group's website.

Glycopeptide Enrichment—Conditioned media were desalted via the use of Zeba spin columns (Thermo Scientific). Proteins were then reduced by 5 mM DTT and alkylated with 25 mM iodoacetamide. After acetone precipitation overnight, the pellet was resuspended in 100 mM triethylammonium bicarbonate (pH 8.5, Sigma) and digested with modified trypsin (Promega) at 37 °C overnight. Peptides were labeled at a ratio of 100 μg peptides/0.8 mg Tandem Mass Tag Zero (TMT^0) (Thermo Scientific) according to the manufacturer's instruction. Labeled peptides were further enriched for glycopeptides using zwitterionic hydrophilic interaction liquid chromatography resin (Merck) (23).

LC/MS of Intact Glycopeptides—The glycopeptide enriched fraction was separated using the EASY-nLC™ nano-HPLC system (Thermo Scientific) with a Magic C18 spray tip 15 cm $\times$ 75 μm inner diameter column (Bruker-Michrom, Auburn, CA). Gradient elution was performed with 4% to 30% acetonitrile in 0.1% formic acid over 60 min at a flow rate of 300 nl/min. The samples were analyzed with an Orbitrap Elite hybrid MS with electron-transfer dissociation (ETD) (Thermo Scientific). The following MS and MS/MS settings were used: Fourier transform: MSn automatic gain control target = 5E4; MS/MS = 1 μscans, max ion time = 200 ms; MS = 300–1800 *m/z*, resolution = 60,000 at *m/z* 400, MS target = 1E6; dynamic exclusion = repeat count 1, duration 30 s, exclusion duration 90 s; higher-energy C-trap dissociation (HCD): collision energy = 35%, resolution = 15,000; MSn target ion trap = 1E4, 2 μscans, max ion time = 150 ms; ETD anion automatic gain control target = 2E5, charge-dependent ETD reaction time enabled. For alternating HCD-ETD MS/MS, the top 10 ions were analyzed. For HCD-product-dependent ETD, the top 10 ions were analyzed via HCD, and product-dependent ETD acquisition was triggered by product (oxonium) ions (*m/z* 163.0812 for Hex; *m/z* 204.0864 for HexNAc; *m/z* 138.0554 for HexNAc fragment ion) (24).

Deglycosylation with PNGase F and $H_2{}^{18}O$—Zwitterionic hydrophilic interaction liquid chromatography resin enriched glycopeptides were resuspended in 50 mM ammonium bicarbonate in $H_2{}^{18}O$ (97 atom % ^{18}O, Sigma) and deglycosylated with PNGase F (Sigma) for 4 h at 37 °C. The samples were separated via reverse-phase nano-flow HPLC (PepMap C18, 3 μm, 100 Å, 25 cm $\times$ 75 μm inner diameter column, Thermo Scientific) before analysis on an LTQ Orbitrap XL MS (Thermo Scientific).

Glycoprotein Enrichment and LC/MS—ConA[1] lectin resins (Thermo Scientific) were used to enrich glycoproteins from concentrated conditioned media according to the manufacturer's protocol. The input, glycoprotein-enriched fraction, and flow-through samples were subjected to trypsin digestion. The in-solution digests were separated on a Thermo Scientific Dionex UltiMate 3000 Rapid Separation LC (RSLC) system using a PepMap C18 column (3 μm, 100 Å, 50 cm $\times$ 75 μm inner diameter column, Thermo Scientific). The rapid separation LC system was interfaced to a Q Exactive MS (Thermo Scientific), and samples were analyzed using a top-10 HCD method.

Database Search and Data analysis—The following parameters were used for different experiments.

(i) Gel-LC-MS/MS: Peak lists were generated by Mascot daemon (version 2.3.0, Matrix Science Ltd., London, UK) using extract_msn_com.exe and searched against the UniProt/Swiss-Prot mamma-

[1] The abbreviations used are: ConA, concanavalin A; EC, endothelial cell; ETD, electron-transfer dissociation; GlcNAc, N-acetylglucosamine; HCD, higher-energy C-trap dissociation; Hex, hexose; HexNAc, N-acetylhexosamine; HUVEC, human umbilical vein endothelial cell; PMA, phorbol-12-myristate-13-acetate; PNGase F, peptide: N-glycosidase F; TMT^0, Tandem Mass Tag Zero; vWF, von Willebrand factor.

lian database (version 2012.03, 65,780 entries) using Mascot (version 2.3.01, Matrix Science) with peptide tolerance = 10 ppm, MS/MS tolerance = 0.8 Da, carbamidomethylation of cysteine as a fixed modification, oxidation of methionine as a variable modification, and a maximum of two missed cleavage sites. The search results were loaded into Scaffold software (version 3.6.2, Proteome Software Software, Inc., Portland, OR). A protein probability greater than 99%, a peptide probability greater than 95%, and a minimum number of two peptides per protein were applied as filters to generate the protein list. Bovine contaminant proteins are listed separately.

(ii) PNGase F + $H_2{}^{18}O$ experiment: Thermo Scientific Proteome Discoverer software version 1.3 was used to search against the UniProt/Swiss-Prot mammalian database (version 2012.03) using Mascot (version 2.3.01, Matrix Science) with a peptide tolerance of 10 ppm; an MS/MS tolerance of 0.8 Da; carbamidomethylation of cysteine as a fixed modification; oxidation of methionine, TMT^0 label on lysine and peptide N-terminus, and deamidation (spontaneous deamidation in ordinary water) and O^{18}-deamidation (deglycosylation by PNGase F in $H_2{}^{18}O$) of asparagine as variable modifications; and a maximum of two missed cleavage sites. Proteome Discoverer produced a custom database containing 136 target proteins based on this search.

(iii) Orbitrap Elite MS: Raw files were searched against the 136-protein database (along with reversed proteins as decoys) using Byonic™ (25) with a peptide tolerance of 10 ppm; an MS/MS tolerance of 20 ppm for HCD and 0.6 Da for ETD; the carbamidomethylated cysteine, TMT^0 label on lysine and peptide N-terminus as fixed modifications; and oxidation of methionine, deamidation of asparagine and glutamine, and phosphorylation of serine and threonine as variable modifications. Byonic™ allowed one N-glycan modification on the N-X(not P)-S/T consensus motif per peptide, with mass and composition chosen from its "common human" glycan database containing 350 glycan masses up to 6000 Da. Glycan modifications were verified by the presence of corresponding glycan fragment ions, such as the HexNAc oxonium ion at 204.087 Da in HCD spectra. Peptide sequences were identified by Byonic™ from the ETD spectra and verified manually.

(iv) Q Exactive MS: Raw files were searched against the UniProt/Swiss-Prot human database (version 57.13, 20,266 entries) using Proteome Discoverer (version 1.3, Thermo Scientific) with Mascot (version 2.3.0, Matrix Science) and a peptide tolerance of 10 ppm, an MS/MS tolerance of 10 mmu, carbamidomethylation of cysteine as a fixed modification, oxidation of methionine as a variable modification, and a maximum of two missed cleavage sites.

RESULTS

The Secretome of Activated ECs—HUVECs were stimulated with PMA, a commonly used secretagogue that induces exocytosis of endothelial vesicles. As previously reported (26), the morphology of ECs changes from spindle-shaped to round upon PMA activation, and the rod-shaped Weibel-Palade bodies, unique storage vesicles within ECs containing vWF and many other secreted proteins, fuse with the cell membrane (Fig. 1*A*). In total, the secretomes of 17 primary ECs were analyzed via gel-LC-MS/MS, with or without deglycosylation. Apart from 123 secreted proteins, the conditioned medium of PMA-stimulated ECs was particularly rich in surface antigens and receptors, including many established endothelial markers (Table I). All identified proteins and peptides are listed in supplemental Tables S1 and S2, respectively. The distribution of the frequencies and the cumulated distribution

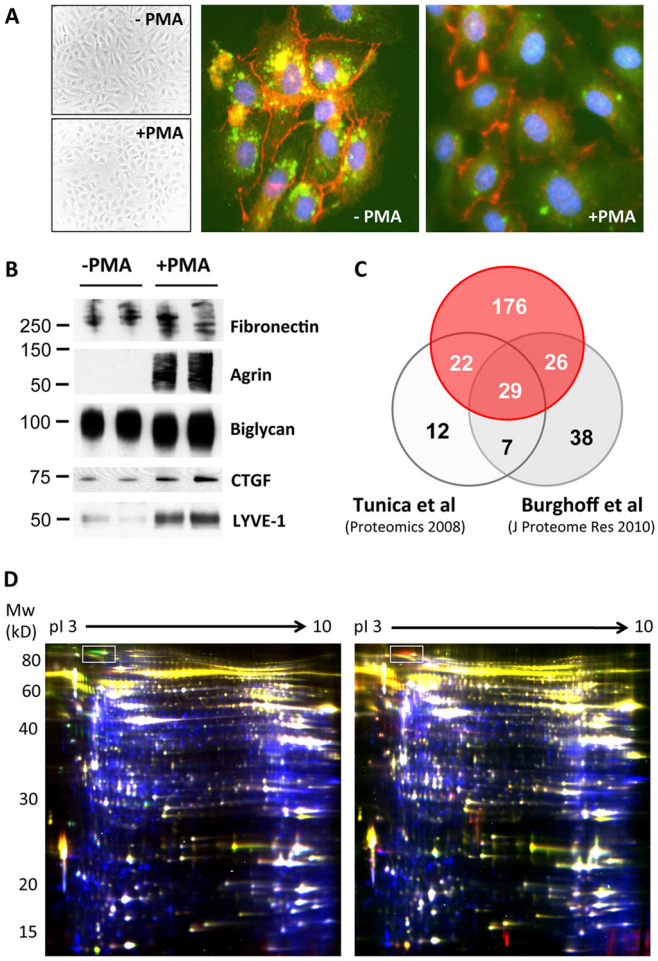

FIG. 1. **PMA treatment to stimulate EC secretion.** Treatment of HUVECs with PMA, a commonly used secretagogue, resulted in a characteristic morphological change indicative of activation. *A*, immunofluorescence staining of vWF (green) and VE-cadherin (red) shows the exocytotic effect of PMA. *B*, PMA increased protein secretion in the conditioned media as confirmed via immunoblotting. *C*, relative to previous studies, more than twice as many secreted and plasma membrane proteins were identified. *D*, overlay of intracellular and secreted proteins by means of difference gel electrophoresis. In the left-hand panel, proteins in conditioned media of HUVECs are stained in green (+PMA) and red (−PMA), and cellular proteins are stained in blue. Results were reproduced with different biological replicates using reverse-labeling (right-hand panel: red, +PMA; green, −PMA). The protein corresponding to von Willebrand antigen 2 is highlighted with a box. Common proteins in the secretome and the cellular proteome are numbered in supplemental Fig. S2 and listed in supplemental Table S3.

of the number of samples in which proteins were identified are shown in supplemental Fig. S1. MS datasets of three biological replicates have been deposited in PRIDE (accession numbers 26908–27003).

Immunoblots confirmed that proteins such as fibronectin and biglycan were constitutively secreted (Fig. 1*B*). Others such as agrin and lymphatic vessel endothelial hyaluronic acid receptor 1 were released upon PMA stimulation, providing an

TABLE I
Extracellular and plasma membrane proteins identified in the HUVEC-conditioned media after PMA stimulation

Protein name	UniProt ID	UniProt accession number	Gene name	Cellular component		Glycoprotein	EC marker
Calcium ion-binding proteins							
Annexin A1	ANXA1_HUMAN	P04083	ANXA1		Plasma membrane		
Annexin A2 [a]	ANXA2_HUMAN	P07355	ANXA2	Extracellular	Plasma membrane		
Annexin A3	ANXA3_HUMAN	P12429	ANXA3		Plasma membrane		
Calreticulin	CALR_HUMAN	P27797	CALR	Extracellular		Glycoprotein	
Calumenin	CALU_HUMAN	O43852	CALU	Extracellular		Glycoprotein	
Calpain-1 catalytic subunit	CAN1_HUMAN	P07384	CAPN1		Plasma membrane		
Calpain-2 catalytic subunit	CAN2_HUMAN	P17655	CAPN2		Plasma membrane		
Calpain small subunit 1	CPNS1_HUMAN	P04632	CAPNS1		Plasma membrane		
Calsyntenin-1	CSTN1_HUMAN	O94985	CLSTN1		Plasma membrane	Glycoprotein	
Calsyntenin-3	CSTN3_HUMAN	Q9BQT9	CLSTN3		Plasma membrane	Glycoprotein	
Desmoglein-1	DSG1_HUMAN	Q02413	DSG1		Plasma membrane	Glycoprotein	
Nucleobindin-2	NUCB2_HUMAN	P80303	NUCB2	Extracellular			
Carbohydrate and glycan metabolism							
Alpha-amylase 1	AMY1_HUMAN	P04745	AMY1C	Extracellular		Glycoprotein	
Exostosin-like 2	EXTL2_HUMAN	Q9UBQ6	EXTL2	Extracellular		Glycoprotein	
Polypeptide N-acetylgalactosaminyltransferase 1	GALT1_HUMAN	Q10472	GALNT1	Extracellular		Glycoprotein	
Sialate O-acetylesterase	SIAE_HUMAN	Q9HAT2	SIAE	Extracellular		Glycoprotein	
UDP-N-acetylhexosamine pyrophosphorylase	UAP1_HUMAN	Q16222	UAP1		Plasma membrane		
Coagulation and related proteins							
Amyloid-like protein 2	APLP2_HUMAN	Q06481	APLP2		Plasma membrane	Glycoprotein	
Multimerin-1	MMRN1_HUMAN	Q13201	MMRN1	Extracellular		Glycoprotein	
Plasminogen activator inhibitor 1	PAI1_HUMAN	P05121	SERPINE1	Extracellular		Glycoprotein	
Plasminogen activator inhibitor 2	PAI2_HUMAN	P05120	SERPINB2	Extracellular		Glycoprotein	
Tissue factor pathway inhibitor	TFPI1_HUMAN	P10646	TFPI	Extracellular		Glycoprotein	
Tissue factor pathway inhibitor 2	TFPI2_HUMAN	P48307	TFPI2	Extracellular		Glycoprotein	
Tissue-type plasminogen activator	TPA_HUMAN	P00750	PLAT	Extracellular		Glycoprotein	
von Willebrand factor	VWF_HUMAN	P04275	VWF	Extracellular		Glycoprotein	EC marker
Extracellular matrix components and associated proteins							
Agrin	AGRIN_HUMAN	O00468	AGRN	Extracellular		Glycoprotein	
Collagen alpha-2(IV) chain	CO4A2_HUMAN	P08572	COL4A2	Extracellular		Glycoprotein	
Collagen alpha-1(VI) chain	CO6A1_HUMAN	P12109	COL6A1	Extracellular		Glycoprotein	
Collagen alpha-1(XII) chain	COCA1_HUMAN	Q99715	COL12A1	Extracellular		Glycoprotein	
Collagen alpha-1(XVIII) chain	COIA1_HUMAN	P39060	COL18A1	Extracellular		Glycoprotein	
EGF-containing fibulin-like extracellular matrix protein 1	FBLN3_HUMAN	Q12805	EFEMP1	Extracellular		Glycoprotein	
Fibrillin-1	FBN1_HUMAN	P35555	FBN1	Extracellular		Glycoprotein	
Fibrillin-2	FBN2_HUMAN	P35556	FBN2	Extracellular		Glycoprotein	
Fibronectin	FINC_HUMAN	P02751	FN1	Extracellular		Glycoprotein	
Hyaluronan and proteoglycan link protein 3	HPLN3_HUMAN	Q96S86	HAPLN3	Extracellular			
Laminin subunit alpha-4	LAMA4_HUMAN	Q16363	LAMA4	Extracellular		Glycoprotein	
Laminin subunit beta-1	LAMB1_HUMAN	P07942	LAMB1	Extracellular		Glycoprotein	
Laminin subunit gamma-1	LAMC1_HUMAN	P11047	LAMC1	Extracellular		Glycoprotein	
Lysyl oxidase homolog 2	LOXL2_HUMAN	Q9Y4K0	LOXL2	Extracellular		Glycoprotein	
Multimerin-2	MMRN2_HUMAN	Q9H8L6	MMRN2	Extracellular		Glycoprotein	

TABLE I—*continued*

Protein name	UniProt ID	UniProt accession number	Gene name	Cellular component		Glycoprotein	EC marker
Nidogen-1	NID1_HUMAN	P14543	NID1	Extracellular		Glycoprotein	
Nidogen-2	NID2_HUMAN	Q14112	NID2	Extracellular		Glycoprotein	
Prolyl 3-hydroxylase 1	P3H1_HUMAN	Q32P28	LEPRE1	Extracellular		Glycoprotein	
Basement membrane-specific heparan sulfate proteoglycan core protein	PGBM_HUMAN	P98160	HSPG2	Extracellular		Glycoprotein	
Biglycan	PGS1_HUMAN	P21810	BGN	Extracellular		Glycoprotein	
Peroxidasin homolog	PXDN_HUMAN	Q92626	PXDN	Extracellular		Glycoprotein	
SPARC	SPRC_HUMAN	P09486	SPARC	Extracellular		Glycoprotein	
Target of Nesh-SH3	TARSH_HUMAN	Q7Z7G0	ABI3BP	Extracellular		Glycoprotein	
Testican-1	TICN1_HUMAN	Q08629	SPOCK1	Extracellular		Glycoprotein	
Thrombospondin-1	TSP1_HUMAN	P07996	THBS1	Extracellular	Plasma membrane	Glycoprotein	
Growth factors and related proteins							
C-type lectin domain family 11 member A	CLC11_HUMAN	Q9Y240	CLEC11A	Extracellular		Glycoprotein	
Cysteine-rich motor neuron 1 protein	CRIM1_HUMAN	Q9NZV1	CRIM1	Extracellular	Plasma membrane	Glycoprotein	
Connective tissue growth factor	CTGF_HUMAN	P29279	CTGF	Extracellular		Glycoprotein	
Protein CYR61, insulin-like growth factor-binding protein 10	CYR61_HUMAN	O00622	CYR61	Extracellular			
Dickkopf-related protein 3	DKK3_HUMAN	Q9UBP4	DKK3	Extracellular		Glycoprotein	
Follistatin-related protein 1	FSTL1_HUMAN	Q12841	FSTL1	Extracellular		Glycoprotein	
Hepatoma-derived growth factor	HDGF_HUMAN	P51858	HDGF	Extracellular			
Insulin-like growth factor-binding protein 2	IBP2_HUMAN	P18065	IGFBP2	Extracellular		Glycoprotein	
Insulin-like growth factor-binding protein 7	IBP7_HUMAN	Q16270	IGFBP7	Extracellular		Glycoprotein	
Latent-transforming growth factor beta-binding protein 1	LTBP1_HUMAN	Q14766	LTBP1	Extracellular		Glycoprotein	
Latent-transforming growth factor beta-binding protein 2	LTBP2_HUMAN	Q14767	LTBP2	Extracellular		Glycoprotein	
Neuronal growth regulator 1	NEGR1_HUMAN	Q7Z3B1	NEGR1		Plasma membrane	Glycoprotein	
Immunity- and inflammation-related proteins							
Amyloid beta A4 protein	A4_HUMAN	P05067	APP	Extracellular	Plasma membrane	Glycoprotein	
Beta-2-microglobulin	B2MG_HUMAN	P61769	B2M	Extracellular		Glycoprotein	
Complement C1q tumor necrosis factor-related protein 5	C1QT5_HUMAN	Q9BXJ0	C1QTNF5	Extracellular			
Complement factor H	CFAH_HUMAN	P08603	CFH	Extracellular		Glycoprotein	
Interleukin-25, UPF0556 protein C19orf10	CS010_HUMAN	Q969H8	C19orf10	Extracellular			
Granulins	GRN_HUMAN	P28799	GRN	Extracellular		Glycoprotein	
Interferon-induced transmembrane protein 1	IFM1_HUMAN	P13164	IFITM1		Plasma membrane		
Galectin-1[a]	LEG1_HUMAN	P09382	LGALS1	Extracellular			
Galectin-3	LEG3_HUMAN	P17931	LGALS3	Extracellular			
Macrophage migration inhibitory factor [a]	MIF_HUMAN	P14174	MIF	Extracellular			
NKG2D ligand 2	N2DL2_HUMAN	Q9BZM5	ULBP2	Extracellular	Plasma membrane	Glycoprotein	
Pentraxin-related protein PTX3	PTX3_HUMAN	P26022	PTX3	Extracellular		Glycoprotein	
Protein S100-A7	S10A7_HUMAN	P31151	S100A7	Extracellular			
Protein S100-A8	S10A8_HUMAN	P05109	S100A8	Extracellular	Plasma membrane		
Tubulointerstitial nephritis antigen-like	TINAL_HUMAN	Q9GZM7	TINAGL1	Extracellular		Glycoprotein	
Nuclease-sensitive element-binding protein 1	YBOX1_HUMAN	P67809	YBX1	Extracellular			
Zinc-alpha-2-glycoprotein	ZA2G_HUMAN	P25311	AZGP1	Extracellular		Glycoprotein	

TABLE I—*continued*

Protein name	UniProt ID	UniProt accession number	Gene name	Cellular component		Glycoprotein	EC marker
Membrane antigens and receptors							
HLA class I histocompatibility antigen, A-24 alpha chain	1A24_HUMAN	P05534	HLA-A		Plasma membrane	Glycoprotein	
HLA class I histocompatibility antigen, A-30 alpha chain	1A30_HUMAN	P16188	HLA-A		Plasma membrane	Glycoprotein	
HLA class I histocompatibility antigen, Cw-12 alpha chain	1C12_HUMAN	P30508	HLA-C		Plasma membrane	Glycoprotein	
Alpha-2-macroglobulin receptor-associated protein	AMRP_HUMAN	P30533	LRPAP1	Extracellular	Plasma membrane	Glycoprotein	
Basal cell adhesion molecule	BCAM_HUMAN	P50895	BCAM		Plasma membrane	Glycoprotein	
Complement component C1q receptor	C1QR1_HUMAN	Q9NPY3	CD93		Plasma membrane	Glycoprotein	EC marker
Cadherin-13	CAD13_HUMAN	P55290	CDH13		Plasma membrane	Glycoprotein	
Cadherin-2	CADH2_HUMAN	P19022	CDH2		Plasma membrane	Glycoprotein	
Cadherin-5	CADH5_HUMAN	P33151	CDH5		Plasma membrane	Glycoprotein	EC marker
CD109 antigen	CD109_HUMAN	Q6YHK3	CD109		Plasma membrane	Glycoprotein	
CD166 antigen	CD166_HUMAN	Q13740	ALCAM		Plasma membrane	Glycoprotein	
CD44 antigen	CD44_HUMAN	P16070	CD44		Plasma membrane	Glycoprotein	
CD59 glycoprotein	CD59_HUMAN	P13987	CD59	Extracellular	Plasma membrane	Glycoprotein	
CD9 antigen	CD9_HUMAN	P21926	CD9		Plasma membrane	Glycoprotein	
C-type lectin domain family 14 member A	CLC14_HUMAN	Q86T13	CLEC14A		Plasma membrane	Glycoprotein	
Dystroglycan	DAG1_HUMAN	Q14118	DAG1	Extracellular	Plasma membrane	Glycoprotein	
Endoglin	EGLN_HUMAN	P17813	ENG		Plasma membrane	Glycoprotein	EC marker
Endothelial protein C receptor	EPCR_HUMAN	Q9UNN8	PROCR		Plasma membrane	Glycoprotein	EC marker
Ephrin type-B receptor 4	EPHB4_HUMAN	P54760	EPHB4		Plasma membrane	Glycoprotein	
Endothelial cell-selective adhesion molecule	ESAM_HUMAN	Q96AP7	ESAM		Plasma membrane	Glycoprotein	EC marker
Leucine-rich repeat transmembrane protein FLRT2	FLRT2_HUMAN	O43155	FLRT2		Plasma membrane	Glycoprotein	
Guanine nucleotide-binding protein subunit beta-2-like 1[a]	GBLP_HUMAN	P63244	GNB2L1		Plasma membrane		
HLA class I histocompatibility antigen, alpha chain E	HLAE_HUMAN	P13747	HLA-E		Plasma membrane	Glycoprotein	
Intercellular adhesion molecule 1	ICAM1_HUMAN	P05362	ICAM1	Extracellular	Plasma membrane	Glycoprotein	EC marker
Intercellular adhesion molecule 2	ICAM2_HUMAN	P13598	ICAM2		Plasma membrane	Glycoprotein	EC marker
Integrin alpha-2	ITA2_HUMAN	P17301	ITGA2		Plasma membrane	Glycoprotein	
Integrin alpha-5	ITA5_HUMAN	P08648	ITGA5		Plasma membrane	Glycoprotein	
Integrin alpha-6	ITA6_HUMAN	P23229	ITGA6		Plasma membrane	Glycoprotein	
Integrin beta-1	ITB1_HUMAN	P05556	ITGB1		Plasma membrane	Glycoprotein	EC marker
Protein jagged-1	JAG1_HUMAN	P78504	JAG1		Plasma membrane	Glycoprotein	
Protein jagged-2	JAG2_HUMAN	Q9Y219	JAG2		Plasma membrane	Glycoprotein	
Junctional adhesion molecule A	JAM1_HUMAN	Q9Y624	F11R		Plasma membrane	Glycoprotein	
BTB/POZ domain-containing protein KCTD12	KCD12_HUMAN	Q96CX2	KCTD12		Plasma membrane		
Kinectin	KTN1_HUMAN	Q86UP2	KTN1		Plasma membrane	Glycoprotein	
Lysosome-associated membrane glycoprotein 1	LAMP1_HUMAN	P11279	LAMP1		Plasma membrane	Glycoprotein	
Low-density lipoprotein receptor	LDLR_HUMAN	P01130	LDLR		Plasma membrane	Glycoprotein	
Low-density lipoprotein receptor-related protein 5	LRP5_HUMAN	O75197	LRP5		Plasma membrane	Glycoprotein	
Lymphatic vessel endothelial hyaluronic acid receptor 1	LYVE1_HUMAN	Q9Y5Y7	LYVE1		Plasma membrane	Glycoprotein	EC marker
Hepatocyte growth factor receptor	MET_HUMAN	P08581	MET	Extracellular	Plasma membrane	Glycoprotein	
Cation-independent mannose-6-phosphate receptor	MPRI_HUMAN	P11717	IGF2R		Plasma membrane	Glycoprotein	
C-type mannose receptor 2	MRC2_HUMAN	Q9UBG0	MRC2		Plasma membrane	Glycoprotein	

TABLE I—*continued*

Protein name	UniProt ID	UniProt accession number	Gene name	Cellular component		Glycoprotein	EC marker
Cell surface glycoprotein MUC18	MUC18_HUMAN	P43121	MCAM		Plasma membrane	Glycoprotein	EC marker
Neuroligin-1	NLGN1_HUMAN	Q8N2Q7	NLGN1		Plasma membrane	Glycoprotein	
Neuronal cell adhesion molecule	NRCAM_HUMAN	Q92823	NRCAM		Plasma membrane	Glycoprotein	
Neuropilin-1	NRP1_HUMAN	O14786	NRP1	Extracellular	Plasma membrane	Glycoprotein	
Neuropilin-2	NRP2_HUMAN	O60462	NRP2		Plasma membrane	Glycoprotein	
Neurotrimin	NTRI_HUMAN	Q9P121	NTM		Plasma membrane	Glycoprotein	
Protocadherin-10	PCD10_HUMAN	Q9P2E7	PCDH10		Plasma membrane	Glycoprotein	
Protocadherin-12	PCD12_HUMAN	Q9NPG4	PCDH12		Plasma membrane	Glycoprotein	
Protocadherin gamma-A11	PCDGB_HUMAN	Q9Y5H2	PCDHGA11		Plasma membrane	Glycoprotein	
Protocadherin gamma-A12	PCDGC_HUMAN	O60330	PCDHGA12		Plasma membrane	Glycoprotein	
Protocadherin gamma-B7	PCDGJ_HUMAN	Q9Y5F8	PCDHGB7		Plasma membrane	Glycoprotein	
Protocadherin-1	PCDH1_HUMAN	Q08174	PCDH1		Plasma membrane	Glycoprotein	
Protocadherin-9	PCDH9_HUMAN	Q9HC56	PCDH9		Plasma membrane	Glycoprotein	
Programmed cell death 1 ligand 2	PD1L2_HUMAN	Q9BQ51	PDCD1LG2	Extracellular	Plasma membrane	Glycoprotein	
Platelet endothelial cell adhesion molecule	PECA1_HUMAN	P16284	PECAM1		Plasma membrane	Glycoprotein	EC marker
Plexin-D1	PLXD1_HUMAN	Q9Y4D7	PLXND1		Plasma membrane	Glycoprotein	
Inactive tyrosine-protein kinase 7	PTK7_HUMAN	Q13308	PTK7		Plasma membrane	Glycoprotein	
Receptor-type tyrosine-protein phosphatase delta	PTPRD_HUMAN	P23468	PTPRD		Plasma membrane	Glycoprotein	
Receptor-type tyrosine-protein phosphatase F	PTPRF_HUMAN	P10586	PTPRF		Plasma membrane	Glycoprotein	
Receptor-type tyrosine-protein phosphatase kappa	PTPRK_HUMAN	Q15262	PTPRK		Plasma membrane	Glycoprotein	
Poliovirus receptor	PVR_HUMAN	P15151	PVR	Extracellular	Plasma membrane	Glycoprotein	
Poliovirus receptor-related protein 2	PVRL2_HUMAN	Q92692	PVRL2		Plasma membrane	Glycoprotein	EC marker
Roundabout homolog 1	ROBO1_HUMAN	Q9Y6N7	ROBO1		Plasma membrane	Glycoprotein	
Roundabout homolog 4	ROBO4_HUMAN	Q8WZ75	ROBO4		Plasma membrane	Glycoprotein	
Syndecan-4	SDC4_HUMAN	P31431	SDC4	Extracellular	Plasma membrane	Glycoprotein	
Semaphorin-4D	SEM4D_HUMAN	Q92854	SEMA4D		Plasma membrane	Glycoprotein	
Semaphorin-6B	SEM6B_HUMAN	Q9H3T3	SEMA6B		Plasma membrane	Glycoprotein	
Tyrosine-protein phosphatase non-receptor type substrate 1	SHPS1_HUMAN	P78324	SIRPA		Plasma membrane	Glycoprotein	
Stabilin-1	STAB1_HUMAN	Q9NY15	STAB1		Plasma membrane	Glycoprotein	EC marker
Transferrin receptor protein 1	TFR1_HUMAN	P02786	TFRC	Extracellular	Plasma membrane	Glycoprotein	
Tyrosine-protein kinase receptor Tie-1	TIE1_HUMAN	P35590	TIE1		Plasma membrane	Glycoprotein	
Tyrosine-protein kinase receptor UFO	UFO_HUMAN	P30530	AXL	Extracellular	Plasma membrane	Glycoprotein	
Vascular endothelial growth factor receptor 2	VGFR2_HUMAN	P35968	KDR	Extracellular	Plasma membrane	Glycoprotein	EC marker
Vascular endothelial growth factor receptor 3	VGFR3_HUMAN	P35916	FLT4	Extracellular	Plasma membrane	Glycoprotein	EC marker
Very low-density lipoprotein receptor	VLDLR_HUMAN	P98155	VLDLR		Plasma membrane	Glycoprotein	
Miscellaneous membrane proteins							
Brain acid soluble protein 1	BASP1_HUMAN	P80723	BASP1		Plasma membrane		
DnaJ homolog subfamily B member 4	DNJB4_HUMAN	Q9UDY4	DNAJB4		Plasma membrane		
RNA-binding protein EWS	EWS_HUMAN	Q01844	EWSR1		Plasma membrane		
Nck-associated protein 1	NCKP1_HUMAN	Q9Y2A7	NCKAP1		Plasma membrane		
Na(+)/H(+) exchange regulatory cofactor NHE-RF2	NHRF2_HUMAN	Q15599	SLC9A3R2		Plasma membrane		
Polymerase I and transcript release factor	PTRF_HUMAN	Q6NZI2	PTRF		Plasma membrane		
Serum deprivation-response protein	SDPR_HUMAN	O95810	SDPR		Plasma membrane		
Sushi repeat-containing protein SRPX2	SRPX2_HUMAN	O60687	SRPX2	Extracellular			
Erythrocyte band 7 integral membrane protein	STOM_HUMAN	P27105	STOM		Plasma membrane		

TABLE I—*continued*

Protein name	UniProt ID	UniProt accession number	Gene name	Cellular component		Glycoprotein	EC marker
Miscellaneous secreted proteins							
Peptidyl-glycine alpha-amidating monooxygenase	AMD_HUMAN	P19021	PAM	Extracellular		Glycoprotein	
Angiopoietin-2	ANGP2_HUMAN	O15123	ANGPT2	Extracellular		Glycoprotein	
Endothelin-1	EDN1_HUMAN	P05305	EDN1	Extracellular			
Endothelial cell-specific molecule 1	ESM1_HUMAN	Q9NQ30	ESM1	Extracellular		Glycoprotein	
Protein FAM3C	FAM3C_HUMAN	Q92520	WNT16	Extracellular			
Epididymal secretory protein E1	NPC2_HUMAN	P61916	NPC2	Extracellular		Glycoprotein	
Programmed cell death protein 10	PDC10_HUMAN	Q9BUL8	PDCD10		Plasma membrane		
Prolactin-inducible protein	PIP_HUMAN	P12273	PIP	Extracellular		Glycoprotein	
Sulfhydryl oxidase 1	QSOX1_HUMAN	O00391	QSOX1	Extracellular		Glycoprotein	
Secretoglobin family 1D member 2	SG1D2_HUMAN	O95969	SCGB1D2	Extracellular			
Thioredoxin[a]	THIO_HUMAN	P10599	TXN	Extracellular			
Thymosin beta-4	TYB4_HUMAN	P62328	TMSB4X	Extracellular			
Protease inhibitors							
Cystatin-C	CYTC_HUMAN	P01034	CST3	Extracellular		Glycoprotein	
Leukocyte elastase inhibitor	ILEU_HUMAN	P30740	SERPINB1	Extracellular			
Inter-alpha-trypsin inhibitor heavy chain H2	ITIH2_HUMAN	P19823	ITIH2	Extracellular		Glycoprotein	
Serpin B9	SPB9_HUMAN	P50453	SERPINB9	Extracellular			
Metalloproteinase inhibitor 1	TIMP1_HUMAN	P01033	TIMP1	Extracellular		Glycoprotein	
Metalloproteinase inhibitor 2	TIMP2_HUMAN	P16035	TIMP2	Extracellular			
Proteases							
Angiotensin-converting enzyme	ACE_HUMAN	P12821	ACE	Extracellular	Plasma membrane	Glycoprotein	EC marker
Disintegrin and metalloproteinase domain-containing protein 10	ADA10_HUMAN	O14672	ADAM10		Plasma membrane	Glycoprotein	
Aminopeptidase B	AMPB_HUMAN	Q9H4A4	RNPEP	Extracellular			
Aminopeptidase N	AMPN_HUMAN	P15144	ANPEP		Plasma membrane	Glycoprotein	
Bone morphogenetic protein 1	BMP1_HUMAN	P13497	BMP1	Extracellular		Glycoprotein	
Cathepsin B	CATB_HUMAN	P07858	CTSB	Extracellular		Glycoprotein	
Cathepsin D	CATD_HUMAN	P07339	CTSD	Extracellular		Glycoprotein	
Cathepsin Z	CATZ_HUMAN	Q9UBR2	CTSZ	Extracellular		Glycoprotein	
Carboxypeptidase Q	CBPQ_HUMAN	Q9Y646	CPQ	Extracellular		Glycoprotein	
Dipeptidyl peptidase 2	DPP2_HUMAN	Q9UHL4	DPP7	Extracellular		Glycoprotein	
Dipeptidyl peptidase 3	DPP3_HUMAN	Q9NY33	DPP3		Plasma membrane		
Endoplasmic reticulum aminopeptidase 1	ERAP1_HUMAN	Q9NZ08	ERAP1	Extracellular		Glycoprotein	
Furin	FURIN_HUMAN	P09958	FURIN		Plasma membrane	Glycoprotein	
Gamma-glutamyl hydrolase	GGH_HUMAN	Q92820	GGH	Extracellular		Glycoprotein	
Serine protease HTRA1	HTRA1_HUMAN	Q92743	HTRA1	Extracellular			
Insulin-degrading enzyme	IDE_HUMAN	P14735	IDE	Extracellular	Plasma membrane		
Interstitial collagenase	MMP1_HUMAN	P03956	MMP1	Extracellular		Glycoprotein	
Stromelysin-2	MMP10_HUMAN	P09238	MMP10	Extracellular			
Matrix metalloproteinase-14	MMP14_HUMAN	P50281	MMP14		Plasma membrane		
72 kDa type IV collagenase	MMP2_HUMAN	P08253	MMP2	Extracellular		Glycoprotein	
Lysosomal Pro-X carboxypeptidase	PCP_HUMAN	P42785	PRCP		Plasma membrane	Glycoprotein	
Serine protease 23	PRS23_HUMAN	O95084	PRSS23	Extracellular		Glycoprotein	
Ubiquitin carboxyl-terminal hydrolase 14	UBP14_HUMAN	P54578	USP14		Plasma membrane		

TABLE I—*continued*

Protein name	UniProt ID	UniProt accession number	Gene name	Cellular component		Glycoprotein	EC marker
Signal transduction proteins							
Adenylyl cyclase-associated protein 1	CAP1_HUMAN	Q01518	CAP1		Plasma membrane		
Cell division control protein 42 homolog	CDC42_HUMAN	P60953	CDC42		Plasma membrane		
Contactin-associated protein-like 3	CNTP3_HUMAN	Q9BZ76	CNTNAP3	Extracellular	Plasma membrane	Glycoprotein	
Adapter molecule crk	CRK_HUMAN	P46108	CRK		Plasma membrane		
Ras GTPase-activating protein-binding protein 1	G3BP1_HUMAN	Q13283	G3BP1		Plasma membrane		
Growth arrest-specific protein 6	GAS6_HUMAN	Q14393	GAS6	Extracellular		Glycoprotein	
Interferon-induced guanylate-binding protein 1	GBP1_HUMAN	P32455	GBP1	Extracellular			
Guanine nucleotide-binding protein G(i) subunit alpha-2	GNAI2_HUMAN	P04899	GNAI2		Plasma membrane		
Glypican-1	GPC1_HUMAN	P35052	GPC1	Extracellular	Plasma membrane	Glycoprotein	
Hedgehog-interacting protein	HHIP_HUMAN	Q96QV1	HHIP	Extracellular	Plasma membrane	Glycoprotein	
Histidine triad nucleotide-binding protein 1[a]	HINT1_HUMAN	P49773	HINT1		Plasma membrane		
Integrin-linked protein kinase	ILK_HUMAN	Q13418	ILK		Plasma membrane		
Ras GTPase-activating-like protein IQGAP1	IQGA1_HUMAN	P46940	IQGAP1		Plasma membrane		
cAMP-dependent protein kinase type II-alpha regulatory subunit	KAP2_HUMAN	P13861	PRKAR2A		Plasma membrane		
Ras-related protein Rab-18	RAB18_HUMAN	Q9NP72	RAB18		Plasma membrane		
Ras-related protein Rab-5C	RAB5C_HUMAN	P51148	RAB5C		Plasma membrane		
Ras-related C3 botulinum toxin substrate 1	RAC1_HUMAN	P63000	RAC1		Plasma membrane		
Ras-related protein Ral-A	RALA_HUMAN	P11233	RALA		Plasma membrane		
Ras-related protein Rap-1b	RAP1B_HUMAN	P61224	RAP1B		Plasma membrane		
GTPase NRas	RASN_HUMAN	P01111	NRAS		Plasma membrane		
Ras-related protein Rab-11A	RB11A_HUMAN	P62491	RAB11A		Plasma membrane		
Rho-related GTP-binding protein RhoC	RHOC_HUMAN	P08134	RHOC		Plasma membrane		
Rho-associated protein kinase 2	ROCK2_HUMAN	O75116	ROCK2		Plasma membrane		
Ras-related protein R-Ras2	RRAS2_HUMAN	P62070	RRAS2		Plasma membrane		
Protein S100-A6[a]	S10A6_HUMAN	P06703	S100A6		Plasma membrane		
Protein S100-A10[a]	S10AA_HUMAN	P60903	S100A10		Plasma membrane		
Switch-associated protein 70	SWP70_HUMAN	Q9UH65	SWAP70		Plasma membrane		
NEDD8-activating enzyme E1 regulatory subunit	ULA1_HUMAN	Q13564	NAE1		Plasma membrane		
Transport-related proteins							
AP-2 complex subunit alpha-1	AP2A1_HUMAN	O95782	AP2A1		Plasma membrane		
AP-2 complex subunit alpha-2	AP2A2_HUMAN	O94973	AP2A2		Plasma membrane		
ADP-ribosylation factor 1	ARF1_HUMAN	P84077	ARF1		Plasma membrane		
ADP-ribosylation factor 6	ARF6_HUMAN	P62330	ARF6		Plasma membrane		
ADP-ribosylation factor-like protein 3	ARL3_HUMAN	P36405	ARL3		Plasma membrane		
Beta-arrestin-1	ARRB1_HUMAN	P49407	ARRB1		Plasma membrane		
Chloride intracellular channel protein 1	CLIC1_HUMAN	O00299	CLIC1		Plasma membrane		
Chloride intracellular channel protein 4	CLIC4_HUMAN	Q9Y696	CLIC4		Plasma membrane		
Clusterin	CLUS_HUMAN	P10909	CLU	Extracellular		Glycoprotein	
Coatomer subunit beta	COPB_HUMAN	P53618	COPB1		Plasma membrane		
EH domain-containing protein 1	EHD1_HUMAN	Q9H4M9	EHD1		Plasma membrane		
EH domain-containing protein 2	EHD2_HUMAN	Q9NZN4	EHD2		Plasma membrane		
Palmitoyl-protein thioesterase 1	PPT1_HUMAN	P50897	PPT1	Extracellular		Glycoprotein	
Protein S100-A13	S10AD_HUMAN	Q99584	S100A13	Extracellular			

TABLE I—*continued*

Protein name	UniProt ID	UniProt accession number	Gene name	Cellular component	Glycoprotein	EC marker
Solute carrier family 12 member 2	S12A2_HUMAN	P55011	SLC12A2	Plasma membrane		
Proactivator polypeptide	SAP_HUMAN	P07602	PSAP	Extracellular	Glycoprotein	
Syntaxin-binding protein 1	STXB1_HUMAN	P61764	STXBP1	Plasma membrane		
Syntaxin-binding protein 3	STXB3_HUMAN	O00186	STXBP3	Plasma membrane		
Transmembrane emp24 domain-containing protein 10	TMEDA_HUMAN	P49755	TMED10	Plasma membrane	Glycoprotein	
Vesicle-associated membrane protein-associated protein A	VAPA_HUMAN	Q9P0L0	VAPA	Plasma membrane		

[a] *These proteins were also identified in the cellular proteome according to the difference gel electrophoresis analysis presented in the supplemental data.*

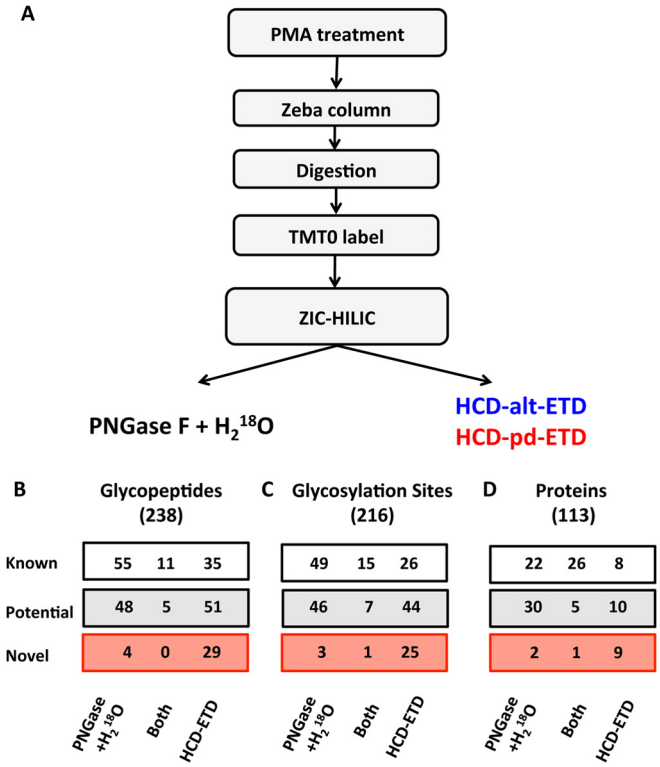

FIG. 2. **Glycoproteomics.** *A*, glycopeptide identification workflow. Comparison of direct and indirect glycopeptide detection using HCD-ETD and ^{18}O-deamidation after PNGase F + $H_2{}^{18}O$ treatment, respectively: identified unique glycopeptides (*B*), unique glycosylation sites (*C*), and unique glycoproteins (*D*).

explanation for why previously unidentified proteins (8, 10) were found in the present analysis (Fig. 1*C*). An overlay between secreted (Cy3 and Cy 5; green and red color) and cellular (Cy 2; blue color) proteins is shown in Fig. 1*D*. Common spots were numbered (supplemental Fig. S2) and identified via LC-MS/MS (supplemental Table S3). Certain proteins, such as von Willebrand antigen 2 (a propeptide of vWF, AA 23–763), were clearly more abundant in the secretome of PMA-treated HUVECs.

The Endothelial Glycoproteome—Among the 1252 identified proteins were 253 extracellular or plasma membrane proteins (approximately 20%) related to cell adhesion, blood coagulation, hemostasis, signaling transduction, and protein transportation, of which 166 were known glycoproteins (Table I). To further characterize this subproteome, we employed a glycoproteomics approach. Secreted proteins were precipitated and digested with trypsin, and tryptic peptides were labeled with TMT^0 to increase their charge state prior to enrichment by means of zwitterionic hydrophilic interaction liquid chromatography purification (24). For glycosite identification, an indirect and a direct strategy were pursued (Fig. 2*A*): (i) digestion with PNGase F in the presence of ^{18}O water to label the conversion of asparagine to aspartic acid upon the removal of N-glycans, and (ii) alternating HCD and ETD (HCD-

alt-ETD) or HCD-product-dependent ETD (HCD-pd-ETD) fragmentation on an Orbitrap Elite MS (24).

There was little overlap in the numbers of glycopeptides (Fig. 2*B*) and glycosylation sites (Fig. 2*C*) identified via the direct (HCD-ETD) and the indirect (PNGase F + $H_2{}^{18}O$) methods. Better agreement was observed at the protein level (Fig. 2*D*). With the indirect (PNGase F + $H_2{}^{18}O$) method, 27 peptides were identified with N[+2.99] modification at non-consensus sequence, out of 1139 total identified peptides with N[+2.99]. This anomaly rate of 2.4% (27/1139) combines the rate of false identifications and the rate of chance deamidations in ^{18}O water that were not in the consensus sequence of glycosylation (*i.e.* N-X(not P)-S/T). All glycopeptides identified are listed in Table II and supplemental Table S4. Three spectra (full MS, HCD, and ETD) from a neuronal cell adhesion molecule (UniProt accession number Q92823) (AA - $_{222}$FNHTQTIQQK$_{231}$) are presented in Fig. 3.

For the same samples, HCD-pd-ETD revealed 28 known, 25 potential, and 16 novel glycosylation sites based on 209 identified spectra; HCD-alt-ETD revealed 20 known, 32 potential, and 14 novel glycosylation sites from 110 identified spectra. The HCD-alt-ETD method selected mostly precursors with higher intensities, higher charge, and smaller *m/z* (Fig. 4*A*). Several large glycopeptides were detected via only HCD-alt-ETD, and more low-abundant glycopeptides were detected via HCD-pd-ETD. There was limited overlap in the identified glycopeptides but better agreement in the protein level (Fig. 4*B*). Among the 319 total glycopeptides identified in the conditioned media, 31 were attached with a trimannosyl core (-$HexNAc_2Hex_3$) or truncated core (-$HexNAc_2Hex$), 50 with high mannose (-$HexNAc_2Hex_{4-9}$), and 238 with complex/hybrid glycans. Notably, HCD-pd-ETD detected almost twice as many complex/hybrid glycoforms as HCD-alt-ETD (Fig.4*C*).

Validation of Glycoproteins—To validate the glycosylation status, we performed additional analysis before and after glycoprotein enrichment with affinity resins of ConA lectin ($n = 4$) using a Q Exactive MS (Thermo Scientific). We then compared the number of identified spectra in the glycoprotein-enriched fraction, the flow-through, and the input (supplemental Table S5). For most glycoproteins, a higher spectral count was observed in the glycoprotein-enriched fraction than in the original input and/or the flow-through. Representative examples (fibronectin, neuronal cell adhesion molecule, tyrosine-protein-kinase-like 7, and vWF) are shown in Fig. 5*A*. Non-glycosylated proteins, such as annexin A2 and alpha-enolase, were more abundant in the flow-through. Glycoproteins identified in all three methods are highlighted in Fig. 5*B*.

Confirmation of Predicted Glycosylation Sites—The hemostatic protein vWF is the main protein stored within Weibel-Palade bodies (27). After secretagogue stimulation, Weibel-Palade bodies undergo exocytosis, releasing vWF filaments. vWF is one of the few known proteins containing the ABO blood group signature, which is formed by different glycans. Although the released glycan composition of this protein has been investigated extensively (28, 29), experimental evidence for many putative glycosylation sites is still missing. The coverage obtained for vWF in our proteomics analysis is shown in Fig. 6*A*. The precursor protein consists of homologous units such as the VWF type A, C, and D domains and a C-terminal cystine know (CTCK). The vWF propeptide (D1-D2, AA 23–763) is separated from the remaining domains of mature vWF (AA 764–2813) via furin-mediated proteolytic cleavage. We confirmed 6 N-glycosylation sites. Notably, three N-glycosylation sites were located within the propeptide (AA 23–763). Examples of ETD spectra are shown in Fig. 6*B*.

DISCUSSION

This study represents a significant advance over the existing proteomics literature on ECs. Unlike other cell types, ECs do not tolerate prolonged serum starvation, and their susceptibility to cell death upon serum withdrawal poses a major challenge for proteomic workflows targeting their secretome. We performed secretome analysis after 45 min of PMA stimulation combined with enrichment strategies for glycoproteins and glycopeptides. Glycopeptides were analyzed via three complementary MS techniques: the detection of ^{18}O asparagine deamidation after digestion with PNGase F in $H_2{}^{18}O$, HCD-alt-ETD, and HCD-pd-ETD using an Orbitrap Elite MS.

The Endothelial Secretome—The secretagogue PMA minimized EC death by allowing a shorter incubation period under serum-free conditions while increasing coverage in the proteomic analysis by inducing the exocytosis of intracellular storage vesicles (14) such as Weibel-Palade bodies. These unique storage vesicles in ECs play a major role in hemostasis and cell-to-cell communication. Using this approach, many more proteins were identified than in any previous proteomics study on ECs, including known endothelial surface markers such as endoglin (CD105), integrin beta-1 (CD29), tyrosine-protein kinase receptor Tie-1, and junctional adhesion molecule A; secreted growth factors (*i.e.* C-type lectin domain family 11 member A); co-receptors (*i.e.* neuropilin-1 (co-receptor for VEGF-A)); proteases(*i.e.* furin); and inflammatory mediators (*i.e.* macrophage migration inhibitory factor), to name just a few. Short-term PMA treatment does not release microparticles (30), as shedding events make it difficult to discern intracellular from secreted/membrane proteins. In a direct comparison of the cellular proteome and the secretome utilizing difference gel electrophoresis, 70 out of 96 proteins analyzed were present in both samples, representing $<10\%$ of the visible protein spots in the secretome.

Biological Importance of Glycosylation—Glycosylation is key for the stability and solubility of secreted and membrane proteins. It is the most complex post-translational modification (31) and mediates extracellular matrix network assembly, cell–cell interactions, and cell–matrix interactions. Unlike polynucleotides and polypeptides, which have a linear struc-

TABLE II
Glycopeptides identified via the HCD-ETD method

Protein name	UniProt ID	Peptide	Glycosite	Type	Glycans	Observed *m/z*	Z	ΔMass (ppm)
Afamin	AFAM_HUMAN	$DIENFN(+1702.582)^STQk	N33	Known	Hex8HexNAc2	843.359	4	−5.8
Aminopeptidase N	AMPN_HUMAN	$kLN(+892.318)YTLSQGHRVVLR	N128	Known	Hex3HexNAc2	781.916	4	−2.8
		$NAN(+2042.720)^SSPVAsTTPSASATTNPASATTLDQSk	N42	Novel	Hex4HexNAc4NeuAc2	1095.276	5	−0.3
Alpha-N-acetylglucosaminidase	ANAG_HUMAN	$SVYN(+1257.450)cSGEAcRGhNRSPLVR	N503	Potential	Hex4HexNAc3	954.927	4	1.1
Angiopoietin-2	ANGP2_HUMAN	$kIVTATVN(+568.212)NSVLQk	N240	Potential	Hex1HexNAc2	689.645	4	−0.3
		$SGhTTNGIYTLTFPN(+1038.375)STEEIk	N304	Potential	Hex3HexNAc2dHex1	763.565	5	−1.4
Attractin	ATRN_HUMAN	$DLDMFIN(+1241.455)ASk	N1198	Known	Hex3HexNAc3dHex1	948.450	3	6.7
		$GcScFSDWQGPGcSVPVPAN(+1095.397)QSFWTR	N325	Potential	Hex3HexNAc3	1077.708	4	−2.1
		$GcScFSDWQGPGcSVPVPAN(+892.317)QSFWTREEYSnLk	N325	Potential	Hex3HexNAc2	1040.061	5	−2.4
Cadherin-2	CADH2_HUMAN	$EQIARFHLRAHAVDInGNQVENPIDIVINVIDMNDNRPEFLHQVWN(+1751.624)GTVPEGSk	N273	Known	Hex4HexNAc4NeuAc1	930.011	9	2.8
Cadherin-5	CADH5_HUMAN	$EN(+1054.370)^ISEYHLTAVIVDk	N112	Known	Hex4HexNAc2	815.146	4	0.7
		$ELDREVYPWYN(+1241.455)LTVEAk	N442	Known	Hex3HexNAc3dHex1	954.972	4	10.0
CD109 antigen	CD109_HUMAN	$LNLYLDSVN(+1038.375)^ETQFcVNIPAVR	N1355	Novel	Hex3HexNAc2dHex1	938.447	4	1.5
		$kkN(+1540.529)ITk	N279	Potential	Hex7HexNAc2	793.410	4	−0.9
		$QN(+1848.640)^STMFSLTPENSWTPk	N513	Novel	Hex8HexNAc2dHex1	1072.719	4	1.0
CD59 glycoprotein	CD59_HUMAN	$TAVN(+1954.704)^csSDFDAcLITk	N43	Known	Hex4HexNAc5NeuAc1	1077.708	4	9.1
Complement factor I	CFAI_HUMAN	$FLNN(+1054.370)GTcTAEGk	N103	Known	Hex4HexNAc2	939.094	3	−4.0
		$LISN(+3534.244)^cSk	N494	Potential	Hex8HexNAc6dHex1NeuAc3	1207.501	4	5.7
CAP-Gly domain-containing linker protein 1	CLIP1_HUMAN	$GEN(+1257.450)^ASAk	N1263	Novel	Hex4HexNAc3	802.359	3	−1.4
		$GEN(+1784.635)ASAk	N1263	Novel	Hex6HexNAc4	970.437	3	10.7
		$EPSATPPISN(+2188.741)LTk	N187	Novel	Hex11HexNAc2	999.192	4	−6.9
		$ANEN(+1200.428)^ASFLQkSIEDMTVk	N971	Novel	Hex4HexNAc2dHex1	980.724	4	2.6
		$ANEN(+1216.423)^ASFLQkSIEDMTVk	N971	Novel	Hex5HexNAc2	985.232	4	11.0
		$ANEN(+1257.449)ASFLQkSIEDMTVk	N971	Novel	Hex4HexNAc3	989.489	4	8.2
		$ANEN(+1444.534)ASFLQkSIEDMTVk	N971	Novel	Hex3HexNAc4dHex1	1036.764	4	9.3
Ephrin type-A receptor 2	EPHA2_HUMAN	$TASVSIN(+892.317)QTEPPkVRLEGR	N435	Known	Hex3HexNAc2	856.694	4	−0.4
Fibrous sheath-interacting protein 2	FSIP2_HUMAN	$IGWEYESTN(+1751.624)ISR	N1423	Novel	Hex4HexNAc4NeuAc1	858.373	4	0.8
		$TITFSAN(+1362.481)VSSHEhTYk	N1675	Novel	Hex5HexNAc2dHex1	912.923	4	3.0
		$GGIN(+892.318)ISGQGSIISAQVSPTR	N215	Novel	Hex3HexNAc2	1020.509	3	1.5
		$ENSN(+1200.428)FSQLALSNEILLGHkEk	N2216	Novel	Hex4HexNAc2dHex1	708.363	6	6.3
		$mPIEN(+1444.534)LSSIQQk	N2824	Novel	Hex3HexNAc4dHex1	825.398	4	0.8
		$YN(+2204.772)k	N427	Novel	Hex5HexNAc4NeuAc2	1026.779	3	7.7
N-acetylglucosamine-6-sulfatase	GNS_HUMAN	$LVkRLEFTGELN(+2018.708)^NTYIFYTSDnGYHTGQFSLPIDkR	N317	Known	Hex6HexNAc3dHex1NeuAc1	696.027	10	−9.6
		$GPGIkPN(+1540.529)QTSk	N362	Potential	Hex7HexNAc2	835.657	4	−0.8
Golgin subfamily A member 4	GOGA4_HUMAN	$ELEhVN(+1735.630)^LSVk	N1612	Novel	Hex3HexNAc4dHex1NeuAc1	848.139	4	−3.9
		$kELEHVN(+1038.375)LSVk	N1612	Novel	Hex3HexNAc2dHex1	752.648	4	0.8
		$kELEHVN(+1524.534)LSVk	N1612	Novel	Hex6HexNAc2dHex1	874.186	4	−1.6
		$SLQENkN(+1257.450)QSk	N585	Novel	Hex4HexNAc3	777.391	4	10.2
		$TRILELESSLEkSLQENkN(+1216.423)QSk	N585	Novel	Hex5HexNAc2	938.686	5	−2.3
Intercellular adhesion molecule 2	ICAM2_HUMAN	$GSLEVN(+2028.741)^cSTTcNQPEVGGLETSLDk	N47	Known	Hex5HexNAc6	1039.861	5	5.1
		$HYLVSN(+568.212)ISHDTVLQcHFTcSGk	N82	Known	Hex1HexNAc2	905.687	4	−0.6
ICOS ligand	ICOSL_HUMAN	$IARTPSVNIGcclENVLLQQN(+2457.877)LTVGSQTGNDIGER	N225	Potential	Hex8HexNAc5dHex1	724.219	9	−5.4
		$IARTPSVNIGcclENVLLQQN(+2594.937)^LTVGSQTGNDIGER	N225	Potential	Hex4HexNAc6dHex1NeuAc2	667.906	10	0.1
Interleukin-6 receptor subunit beta	IL6RB_HUMAN	$SHLQN(+568.212)YTVNATkLTVNLTNDRYLATLTVRNLVGk	N379	Known	Hex1HexNAc2	725.691	7	6.5

TABLE II—*continued*

Protein name	UniProt ID	Peptide	Glycosite	Type	Glycans	Observed *m/z*	Z	ΔMass (ppm)
		$SHLQN(+568.212)YTVNATkLTVNLTNDRYLATLTVRNLVGk	N379	Known	Hex1HexNAc2	1015.568	5	9.4
		$LTVN(+1460.529)LTNDRYLATLTVRNLVGk	N390	Known	Hex4HexNAc4	877.848	5	−8.4
		$QN(+568.212)cSQHESSPDIsHFER	N818	Novel	Hex1HexNAc2	733.814	4	8.8
Integrin alpha-3	ITA3_HUMAN	$DVRkLLLSIN(+892.317)VTNTR	N656	Potential	Hex3HexNAc2	1028.554	3	−2.2
		$AHcVWLEcPIPDAPVVTN(+1362.481)VTVk	N926	Potential	Hex5HexNAc2dHex1	864.223	5	8.3
Integrin beta-1	ITB1_HUMAN	$kNkNVTN(+1444.534)^RSk	N97	Potential	Hex3HexNAc4dHex1	888.710	4	2.8
Junctional adhesion molecule C	JAM3_HUMAN	$IWN(+1581.555)VTRRDSALYRcEVVARNDR	N104	Potential	Hex6HexNAc3	1139.528	4	−4.8
		$IWN(+892.318)^VTR	N104	Potential	Hex3HexNAc2	643.303	3	−0.7
Lysosome-associated membrane glycoprotein 1	LAMP1_HUMAN	$GHTLTLN(+1378.476)FTR	N103	Known	Hex6HexNAc2	921.421	3	−0.4
		$GHTLTLN(+1540.529)FTR	N103	Known	Hex7HexNAc2	975.439	3	−0.4
		$YNVSGTNGTcLLASMGLQLN(+2042.720)^LTYERkDNT TVTRLLnINPNk	N241	Known	Hex4HexNAc4NeuAc2	734.661	10	6.4
		$kDN(+2059.735)TTVTR	N249	Known	Hex5HexNAc4dHex1NeuAc1	861.641	4	1.0
		$kDN(+2204.772)TTVTR	N249	Known	Hex5HexNAc4NeuAc2	898.156	4	5.8
		$kDN(+2350.830)TTVTR	N249	Known	Hex5HexNAc4dHex1NeuAc2	934.414	4	−0.2
		$kDN(+2569.905)TTVTR	N249	Known	Hex6HexNAc5NeuAc2	989.440	4	6.2
		$kDN(+2570.925)TTVTR	N249	Known	Hex6HexNAc5dHex2NeuAc1	989.690	4	1.0
		$kDN(+2571.946)TTVTR	N249	Known	Hex6HexNAc5dHex4	989.690	4	−2.4
		$kDN(+2715.963)^TTVTR	N249	Known	Hex6HexNAc5dHex1NeuAc2	1031.190	4	−2.0
		$kDN(+2715.963)TTVTR	N249	Known	Hex6HexNAc5dHex1NeuAc2	1025.696	4	−0.9
		$kDN(+2717.978)TTVTR	N249	Known	Hex8HexNAc7	1025.949	4	−1.2
		$kDN(+2861.000)TTVTR	N249	Known	Hex6HexNAc5NeuAc3	1062.211	4	3.1
		$kDN(+2864.036)TTVTR	N249	Known	Hex8HexNAc7dHex1	1062.466	4	1.2
		$kDN(+3007.058)TTVTR	N249	Known	Hex6HexNAc5dHex1NeuAc3	1098.476	4	4.4
		$AAN(+1702.581)GSLR	N322	Known	Hex8HexNAc2	872.711	3	2.6
		$AAN(+1864.634)GSLR	N322	Known	Hex9HexNAc2	926.395	3	3.5
Lysosome-associated membrane glycoprotein 2	LAMP2_HUMAN	$EkPEAGTYSVNNGN(+1054.370)DTcLLATmGLQLNITQDk	N229	Known	Hex4HexNAc2	1048.506	5	0.8
Lysosomal alpha-glucosidase	LYAG_HUMAN	$QVVEN(+1095.397)^MTRAHFPLDVQWNDLDYMDSR	N390	Known	Hex3HexNAc3	905.408	5	0.9
		$GAYTQVIFLARN(+1054.370)NTIVNELVR	N882	Known	Hex4HexNAc2	918.718	4	1.4
Protein-lysine 6-oxidase	LYOX_HUMAN	$AEN(+1054.370)QTAPGEVPALSNLR	N144	Potential	Hex4HexNAc2	762.369	4	8.1
		$DPGAAVPGAANASAQQPRTPILLIRDN(+2432.884)R	N97	Potential	Hex3HexNAc6dHex1NeuAc2	1106.316	5	−5.0
Lymphatic vessel endothelial hyaluronic acid receptor 1	LYVE1_HUMAN	$AN(+1362.481)DSNPNEESkkTDk	N289	Novel	Hex5HexNAc2dHex1	984.727	4	5.8
Lysosomal alpha-mannosidase	MA2B1_HUMAN	$GFkDHFTFcQQLN(+892.317)lSIcPLSQTAARFQVIVYnPLGRk	N497	Potential	Hex3HexNAc2	987.504	6	−1.2
Hepatocyte growth factor receptor	MET_HUMAN	$TLLRN(+1751.624)^SsGcEARRDEYR	N405	Potential	Hex4HexNAc4NeuAc1	1040.946	4	6.4
		$VIVQPDQN(+2042.720)^^FTGLIAGVVSISTALLLLLGFFLWLkkRk	N930	Potential	Hex4HexNAc4NeuAc2	886.225	8	3.5
		$VIVQPDQN(+2174.799)^FTGLIAGVVSISTALLLLLGFFLWLkkR	N930	Potential	Hex5HexNAc6dHex1	1140.772	6	4.0
Interstitial collagenase	MMP1_HUMAN	$AFQLWSN(+2034.703)^VTPLTFTk	N143	Novel	Hex7HexNAc3NeuAc1	1065.992	4	3.1
		$AFQLWSN(+2059.735)VTPLTFTk	N143	Novel	Hex5HexNAc4dHex1NeuAc1	1065.999	4	0.3
		$AFQLWSN(+2075.730)^VTPLTFTk	N143	Novel	Hex6HexNAc4NeuAc1	1076.245	4	0.2
		$AFQLWSN(+2075.730)VTPLTFTk	N143	Novel	Hex5HexNAc4dHex2NeuGc1	1070.250	4	1.4
		$AFQLWSN(+2076.750)VTPLTFTk	N143	Novel	Hex6HexNAc4dHex2	1070.251	4	−1.0
		$AFQLWSN(+2092.745)VTPLTFTk	N143	Novel	Hex7HexNAc4dHex2	1074.251	4	0.2
		$AFQLWSN(+2350.830)^VTPLTFTk	N143	Novel	Hex5HexNAc4dHex1NeuAc2	1144.769	4	−0.3
		$AFQLWSN(+2350.830)VTPLTFTk	N143	Novel	Hex5HexNAc4dHex1NeuAc2	1139.021	4	−1.9
		$AFQLWSN(+2351.851)VTPLTFTk	N143	Novel	Hex5HexNAc4dHex3NeuAc1	1139.277	4	−0.9

TABLE II—*continued*

Protein name	UniProt ID	Peptide	Glycosite	Type	Glycans	Observed *m/z*	Z	ΔMass (ppm)
Multimerin-1	MMRN1_HUMAN	$INALkkPTVN(+1200.428)LTTVLIGR	N1020	Known	Hex4HexNAc2dHex1	957.031	4	1.5
		$GARLFVLLSSLWSGGIGLN(+1241.455)^NSk	N21	Potential	Hex3HexNAc3dHex1	1001.006	4	−3.0
		$LFVLLSSLWSGGIGLN(+568.212)NSk	N21	Potential	Hex1HexNAc2	756.162	4	−0.8
		$IDN(+1095.397)^ISLTVNDVRNTYSSLEGk	N344	Known	Hex3HexNAc3	976.973	4	−1.1
		$InN(+568.212)LTVSLEMEk	N576	Potential	Hex1HexNAc2	803.746	3	−1.8
		$kIEN(+892.317)LTSAVNSLNFIIk	N680	Potential	Hex3HexNAc2	868.469	4	−3.4
		$LNQSNFQkmYQMFN(+2262.815)^ETTSQVR	N828	Potential	Hex5HexNAc5dHex1NeuAc1	1069.470	5	2.0
		$ALEAkSIHLSInFFSLN(+568.212)k	N921	Potential	Hex1HexNAc2	819.195	4	−5.2
		$SIHLSINFFSLN(+892.318)^k	N921	Potential	Hex3HexNAc2	721.609	4	−6.7
C-type mannose receptor 2	MRC2_HUMAN	$VTPAcN(+2059.735)TSLPAQR	N69	Known	Hex5HexNAc4dHex1NeuAc1	925.654	4	−2.1
		$SN(+2059.735)VTk	N954	Potential	Hex5HexNAc4dHex1NeuAc1	1020.122	3	0.2
Nck-associated protein 5	NCKP5_HUMAN	$ERGPQGQGHGRMALNLQLSDTDDN(+2018.708)^ETFDELHIESSDEk	N585	Novel	Hex6HexNAc3dHex1NeuAc1	1127.492	6	−3.7
Lysosomal protein NCU-G1	NCUG1_HUMAN	$LLHTADTcQLEVALIGAsPRGN(+1241.454)R	N230	Potential	Hex3HexNAc3dHex1	1010.223	4	−1.4
Natural cytotoxicity triggering receptor 3 ligand 1	NR3L1_HUMAN	$LN(+2172.745)SSQEDPGTVYQcVVRHASLHTPLR	N216	Potential	Hex10HexNAc2dHex1	1073.477	5	−4.3
Neuronal cell adhesion molecule	NRCAM_HUMAN	$IPAN(+2715.963)k	N1009	Potential	Hex6HexNAc5dHex1NeuAc2	927.404	4	−1.4
		$IPAN(+2960.068)^k	N1009	Potential	Hex5HexNAc7dHex1NeuAc2	1000.181	4	6.5
		$FN(+1378.476)HTQTIQQk	N223	Potential	Hex6HexNAc2	768.611	4	0.9
		$FN(+1378.476)HTQTIQQk	N223	Potential	Hex6HexNAc2	1024.480	3	2.2
		$SSRERPPTFLTPEGN(+1710.598)ASNk	N276	Known	Hex5HexNAc3NeuAc1	1062.994	4	−0.4
Nuclear receptor-interacting protein 3	NRIP3_HUMAN	$LMETN(+568.212)LSk	N72	Novel	Hex1HexNAc2	651.345	3	8.7
Plasminogen activator inhibitor 1	PAI1_HUMAN	$GN(+1694.603)^MTRLPRLLVLPkFSLETEVDLRk	N288	Known	Hex4HexNAc3dHex1NeuAc1	1063.953	5	3.4
		$GN(+2059.735)MTR	N288	Known	Hex5HexNAc4dHex1NeuAc1	955.394	3	0.5
		$GN(+2350.830)^mTR	N288	Known	Hex5HexNAc4dHex1NeuAc2	799.313	4	−3.7
		$GN(+2351.851)^mTR	N288	Known	Hex5HexNAc4dHex3NeuAc1	798.814	4	−5.6
Platelet-derived growth factor subunit B	PDGFB_HUMAN	$LLHGDPGEEDGAELDLN(+1864.634)mTRSHSG GELESLARGRR	N63	Novel	Hex9HexNAc2	1176.921	5	−5.5
Secretory phospholipase A2 receptor	PLA2R_HUMAN	$MQDTSGHGVNTsDMYPMPNTLEYGN(+2204.772)^RTYk	N1123	Novel	Hex5HexNAc4NeuAc2	1014.913	6	−1.9
Procollagen-lysine,2-oxoglutarate 5-dioxygenase 2	PLOD2_HUMAN	$YFN(+1856.656)YTVkVLGQGEEWR	N63	Potential	Hex5HexNAc3dHex1NeuAc1	1074.744	4	0.2
Phospholipid transfer protein	PLTP_HUMAN	$qLLYWFFYDGGYIN(+2157.783)^ASAEGVSIRTGLELSR	N117	Potential	Hex4HexNAc6NeuAc1	1118.898	5	0.2
		$IYSN(+1403.507)HSALESLALIPLQAPLk	N398	Known	Hex4HexNAc3dHex1	1033.782	4	1.5
Plexin-C1	PLXC1_HUMAN	$IAN(+1524.534)^FTSDVEYSDDHchLILPDSEAFQDVQGkRHR	N1308	Novel	Hex6HexNAc2dHex1	1203.342	5	−1.8
		$IAN(+2204.773)FTSDVEYSDDhcHLILPDSEAFQDVQGkR	N1308	Novel	Hex5HexNAc4NeuAc2	638.689	10	5.9
		$VILGEN(+1298.476)LTSNcPEVIYEIk	N407	Known	Hex3HexNAc4	985.483	4	−1.8
		$ELcQN(+1378.476)k	N548	Potential	Hex6HexNAc2	873.730	3	8.0
		$DVcIQFDGGNcSSVGSLSYIALPHcSLIFPATTWISGGQN (+1403.508)^ITMMGR	N771	Potential	Hex4HexNAc3dHex1	607.279	11	0.5
		$ENDNFN(+1054.370)ISk	N871	Novel	Hex4HexNAc2	861.725	3	−4.1
		$ENDNFN(+2522.916)^ISk	N871	Novel	Hex5HexNAc7NeuAc1	1019.438	4	7.5
Tyrosine-protein kinase-like 7	PTK7_HUMAN	$SAN(+3007.058)ASFNIk	N116	Known	Hex6HexNAc5dHex1NeuAc3	1102.722	4	2.1
		$SAN(+3026.090)ASFNIk	N116	Known	Hex9HexNAc7dHex1	1107.479	4	1.3
		$ATVFAN(+1710.598)GSLLLTQVRPR	N283	Known	Hex5HexNAc3NeuAc1	945.458	4	0.0
		$RQDVN(+1686.586)ITVATVPSWLk	N405	Potential	Hex7HexNAc2dHex1	991.485	4	3.2
Pentraxin-related protein PTX3	PTX3_HUMAN	$ATDVLN(+1419.502)kTILFsYGTk	N220	Potential	Hex5HexNAc3	986.474	4	−4.0

TABLE II—*continued*

Protein name	UniProt ID	Peptide	Glycosite	Type	Glycans	Observed *m/z*	Z	ΔMass (ppm)
Proactivator polypeptide	SAP_HUMAN	$TN(+1038.375)STFVQALVEHVk	N215	Known	Hex3HexNAc2dHex1	1020.847	3	1.2
		$LIDNN(+1216.423)kTEk	N332	Known	Hex5HexNAc2	988.825	3	−0.7
		$LIDNN(+1378.476)kTEk	N332	Known	Hex6HexNAc2	1042.510	3	0.7
		$LIDNN(+1694.603)kTEk	N332	Known	Hex4HexNAc3dHex1NeuAc1	861.415	4	−0.8
		$N(+2245.800)ˇSTk	N426	Known	Hex4HexNAc5NeuAc2	1056.113	3	−0.8
		$NLEkN(+1378.476)STk	N426	Known	Hex6HexNAc2	995.485	3	2.5
Histone deacetylase complex subunit SAP30	SAP30_HUMAN	$N(+1095.397)kSDLk	N209	Novel	Hex3HexNAc3	824.751	3	−3.7
		$GGDAAAAVAAVVAAAAAAAsAGN(+1589.571)GTGAG TGAEVPGAGAVSAAGPPGAAGPGPGQLccLR	N34	Novel	Hex3HexNAc4NeuAc1	682.815	10	−0.7
Serpin H1	SERPH_HUMAN	$SLSN(+1378.476)ˇSTAR	N120	Potential	Hex6HexNAc2	821.017	3	−1.4
		$SLSN(+1378.476)STAR	N120	Potential	Hex6HexNAc2	813.358	3	1.9
		$SLSN(+1540.529)STAR	N120	Potential	Hex7HexNAc2	867.371	3	−3.6
		$SLSN(+1702.581)STAR	N120	Potential	Hex8HexNAc2	922.062	3	1.6
		$SLSN(+1864.634)STAR	N120	Potential	Hex9HexNAc2	975.414	3	4.5
		$N(+1540.529)VTWk	N125	Potential	Hex7HexNAc2	879.399	3	−0.5
		$N(+1702.581)VTWk	N125	Potential	Hex8HexNAc2	933.418	3	0.6
Tyrosine-protein phosphatase non-receptor type substrate 1	SHPS1_HUMAN	$LQLTWLEnGN(+1200.428)VSR	N292	Known	Hex4HexNAc2dHex1	739.847	4	−3.5
		$LQLTWLENGN(+1872.651)ˇVSR	N292	Known	Hex6HexNAc3NeuAc1	912.893	4	−11.5
SPARC	SPRC_HUMAN	$VcSNDN(+1622.582)k	N116	Known	Hex5HexNAc4	970.425	3	3.5
		$VcSNDN(+1767.619)k	N116	Known	Hex4HexNAc4NeuGc1	1019.107	3	4.9
		$VcSNDN(+1768.640)k	N116	Known	Hex5HexNAc4dHex1	1018.439	3	0.0
		$VcSNDN(+1864.634)k	N116	Known	Hex9HexNAc2	1051.108	3	2.2
		$VcSNDN(+1913.677)ˇk	N116	Known	Hex5HexNAc4NeuAc1	806.336	4	−1.4
		$VcSNDN(+1913.677)k	N116	Known	Hex5HexNAc4NeuAc1	800.591	4	−0.3
		$VcSNDN(+1913.677)k	N116	Known	Hex5HexNAc4NeuAc1	1066.783	3	−1.7
		$VcSNDN(+1914.697)k	N116	Known	Hex5HexNAc4dHex2	800.844	4	−2.5
		$VcSNDN(+1914.697)k	N116	Known	Hex5HexNAc4dHex2	1067.125	3	0.6
		$VcSNDN(+2059.735)ˇk	N116	Known	Hex5HexNAc4dHex1NeuAc1	842.598	4	−3.0
		$VcSNDN(+2059.735)k	N116	Known	Hex5HexNAc4dHex1NeuAc1	836.857	4	3.1
		$VcSNDN(+2059.735)k	N116	Known	Hex5HexNAc4dHex1NeuAc1	1115.472	3	1.6
		$VcSNDN(+2350.830)k	N116	Known	Hex5HexNAc4dHex1NeuAc2	909.629	4	0.3
Stabilin-1	STAB1_HUMAN	$ELLQHHGLVPQIEAATAYTIFVPTnRSLEAQGN (+2366.825)ˇSSHLDADTVR	N1178	Potential	Hex6HexNAc4NeuAc2	732.443	10	3.2
		$ELkGDGPFTIFVPHADLMSN(+568.212)LSQDELARIR	N1626	Known	Hex1HexNAc2	1097.310	4	−5.4
		$LLPAHsGLSLIISDAGPDN(+892.317)SSWAPVAPGTVVVSR	N2424	Known	Hex3HexNAc2	655.464	7	−7.8
		$ILTMAnQVLAVN(+1095.397)ISEEGR	N606	Potential	Hex3HexNAc3	820.390	4	−9.4
		$GN(+1216.423)cSDGIQGNGAcLcFPDYk	N745	Potential	Hex5HexNAc2	975.155	4	−10.2
Suppressor of G2 allele of SKP1 homolog	SUGT1_HUMAN	$RAMN(+568.212)kSFMESGGTVLSTNWsDVGk	N329	Novel	Hex1HexNAc2	981.480	4	6.2
Angiopoietin-1 receptor	TIE2_HUMAN	$ISN(+568.212)ITHSSAVIsWTILDGYSISSITIR	N649	Potential	Hex1HexNAc2	762.382	5	−3.1
Tetraspanin-3	TSN3_HUMAN	$TYN(+1825.661)GTNPDAASRAIDYVQR	N127	Potential	Hex5HexNAc5	1041.454	4	−7.9
Thrombospondin-1	TSP1_HUMAN	$VVN(+1913.677)STTGPGEHLR	N1067	Known	Hex5HexNAc4NeuAc1	877.141	4	0.2
Vascular endothelial growth factor receptor 1	VGFR1_HUMAN	$RIIWDSRkGFIISN(+892.317)ATYk	N196	Potential	Hex3HexNAc2	934.508	4	8.1
		$SVN(+892.318)TSVhIYDkAFITVk	N323	Potential	Hex3HexNAc2	876.466	4	10.2
		$WFWHPcNHN(+1419.502)HSEARcDFcSNNEESFIL DADSnMGNR	N474	Potential	Hex5HexNAc3	1017.415	6	1.3
		$mAITkEhSITLNLTIMN(+1257.450)ˇVSLQDSGTYAcRAR	N625	Potential	Hex4HexNAc3	1051.702	5	−0.2

TABLE II—*continued*

Protein name	UniProt ID	Peptide	Glycosite	Type	Glycans	Observed *m/z*	Z	ΔMass (ppm)
von Willebrand factor	VWF_HUMAN	$YFN(+2059.735)^k	N156	Potential	Hex5HexNAc4dHex1NeuAc1	776.330	4	−4.7
		$YFN(+2059.735)^k	N156	Potential	Hex5HexNAc4dHex1NeuAc1	1034.440	3	−1.2
		$YFN(+2059.735)k	N156	Potential	Hex5HexNAc4dHex1NeuAc1	1027.114	3	−0.1
		$YFN(+2059.736)k	N156	Potential	Hex5HexNAc4dHex1NeuAc1	770.587	4	−0.6
		$YFN(+2204.772)k	N156	Potential	Hex5HexNAc4NeuAc2	1075.798	3	3.0
		$YFN(+2221.789)k	N156	Potential	Hex6HexNAc4dHex1NeuAc1	1081.467	3	0.8
		$YFN(+2350.830)^^k	N156	Potential	Hex5HexNAc4dHex1NeuAc2	854.851	4	−3.2
		$YFN(+2350.830)^k	N156	Potential	Hex5HexNAc4dHex1NeuAc2	848.856	4	−0.9
		$YFN(+2350.830)^k	N156	Potential	Hex5HexNAc4dHex1NeuAc2	1131.473	3	−0.2
		$YFN(+2350.830)k	N156	Potential	Hex5HexNAc4dHex1NeuAc2	843.362	4	0.5
		$YFN(+2350.830)k	N156	Potential	Hex5HexNAc4dHex1NeuAc2	1124.145	3	−0.7
		$YFN(+2350.831)^k	N156	Potential	Hex5HexNAc4dHex1NeuAc2	848.857	4	0.0
		$YFN(+2350.831)k	N156	Potential	Hex5HexNAc4dHex1NeuAc2	843.362	4	1.2
		$YFN(+2351.851)^k	N156	Potential	Hex5HexNAc4dHex3NeuAc1	849.613	4	−0.2
		$YFN(+2366.825)^k	N156	Potential	Hex5HexNAc4dHex1NeuAc1 NeuGc1	853.098	4	−9.4
		$YFN(+2366.825)k	N156	Potential	Hex5HexNAc4dHex1NeuAc1 NeuGc1	1129.813	3	0.5
		$YFN(+2715.963)^k	N156	Potential	Hex6HexNAc5dHex1NeuAc2	940.387	4	−3.7
		$YFN(+2715.963)k	N156	Potential	Hex6HexNAc5dHex1NeuAc2	934.643	4	−0.8
		$YFN(+2716.983)k	N156	Potential	Hex6HexNAc5dHex3NeuAc1	934.898	4	−1.5
		$YFN(+2861.001)k	N156	Potential	Hex6HexNAc5NeuAc3	971.409	4	3.7
		$YFN(+3007.058)k	N156	Potential	Hex6HexNAc5dHex1NeuAc3	1007.667	4	−2.2
		$YFN(+3009.074)k	N156	Potential	Hex8HexNAc7	1007.923	4	0.6
		$YFN(+3026.089)k	N156	Potential	Hex9HexNAc7dHex1	1012.676	4	−2.0
		$YFN(+3372.190)k	N156	Potential	Hex7HexNAc6dHex1NeuAc3	1098.951	4	−0.9
		$GDILQRVREIRYQGGN(+1378.476)R	N1574	Known	Hex6HexNAc2	909.439	4	−0.2
		$GDILQRVREIRYQGGN(+568.212)RTNTGLALR	N1574	Known	Hex1HexNAc2	912.984	4	−4.0
		$YQGGN(+2059.735)R	N1574	Known	Hex5HexNAc4dHex1NeuAc1	993.411	3	1.2
		$ASPPSSScN(+2059.735)ISSGEmQk	N211	Potential	Hex5HexNAc4dHex1NeuAc1	1073.955	4	−2.4
		$ASPPSSScN(+2350.830)^ISSGEmQk	N211	Potential	Hex5HexNAc4dHex1NeuAc2	1151.736	4	8.9
		$ASPPSSScN(+2350.830)ISSGEmQk	N211	Potential	Hex5HexNAc4dHex1NeuAc2	1146.231	4	0.3
		$N(+2059.735)VScPQLEVPVcPSGFQLSck	N2546	Known	Hex5HexNAc4dHex1NeuAc1	984.037	5	−3.6
		$GQVYLQcGTPcN(+2059.735)LTcR	N666	Potential	Hex5HexNAc4dHex1NeuAc1	1053.444	4	0.9
		$GQVYLQcGTPcN(+2075.730)LTcR	N666	Potential	Hex6HexNAc4NeuAc1	1057.695	4	2.2
		$GQVYLQcGTPcN(+2076.750)LTcR	N666	Potential	Hex6HexNAc4dHex2	1058.193	4	−0.6
		$GQVYLQcGTPcN(+2350.830)LTcR	N666	Potential	Hex5HexNAc4dHex1NeuAc2	1126.222	4	4.5
Bovine proteins								
Alpha-1-acid glycoprotein	A1AG_BOVIN	$QN(+2861.000)^GTLSk	N104	Potential	Hex6HexNAc5NeuAc3	1020.428	4	0.4
		$QN(+2861.000)GTLSk	N104	Potential	Hex6HexNAc5NeuAc3	1014.934	4	1.8
		$QN(+2880.031)GTLSk	N104	Potential	Hex9HexNAc7	1019.690	4	0.5
		$NPEYN(+2814.010)^^k	N57	Potential	Hex5HexNAc7NeuAc2	1018.923	4	6.2
Alpha-fetoprotein	FETA_BOVIN	$AEN(+1200.428)ATEcFETk	N197	Potential	Hex4HexNAc2dHex1	983.428	3	−5.8
		$AEN(+2204.772)ATEcFETk	N197	Potential	Hex5HexNAc4NeuAc2	988.913	4	0.1
		$AN(+2204.772)FTEIQk	N251	Potential	Hex5HexNAc4NeuAc2	901.651	4	2.5
Alpha-2-HS-glycoprotein	FETUA_BOVIN	$kLcPDcPLLAPLN(+2204.772)DSR	N156	Known	Hex5HexNAc4NeuAc2	905.409	5	0.3
		$kLcPDcPLLAPLN(+2861.000)DSR	N156	Known	Hex6HexNAc5NeuAc3	1036.654	5	−1.0
		$LcPDcPLLAPLN(+2204.772)DSR	N156	Known	Hex5HexNAc4NeuAc2	1043.195	4	−1.7

Peptide modification symbols: $, N-terminal TMT0 labelling (+224.152); ^, Na adduct on glycan (+21.982); ^^, 2 Na adduct on glycan (+43.964); c, carbamidomethylation of cysteine (+57.021); h, oxidation of histidine (+15.995); k, TMT^0 labeling of lysine (+224.152); m, oxidation of methionine (+15.995); n, deamidation of asparagine (+0.984); q, Gln->pyro-Glu and loss of TMT^0 (−241.179); s, phosphorylation of serine (+79.966).

Underlined glycopeptides were also detected via the PNGase F + $H_2{}^{18}O$ method (supplemental Table S4).

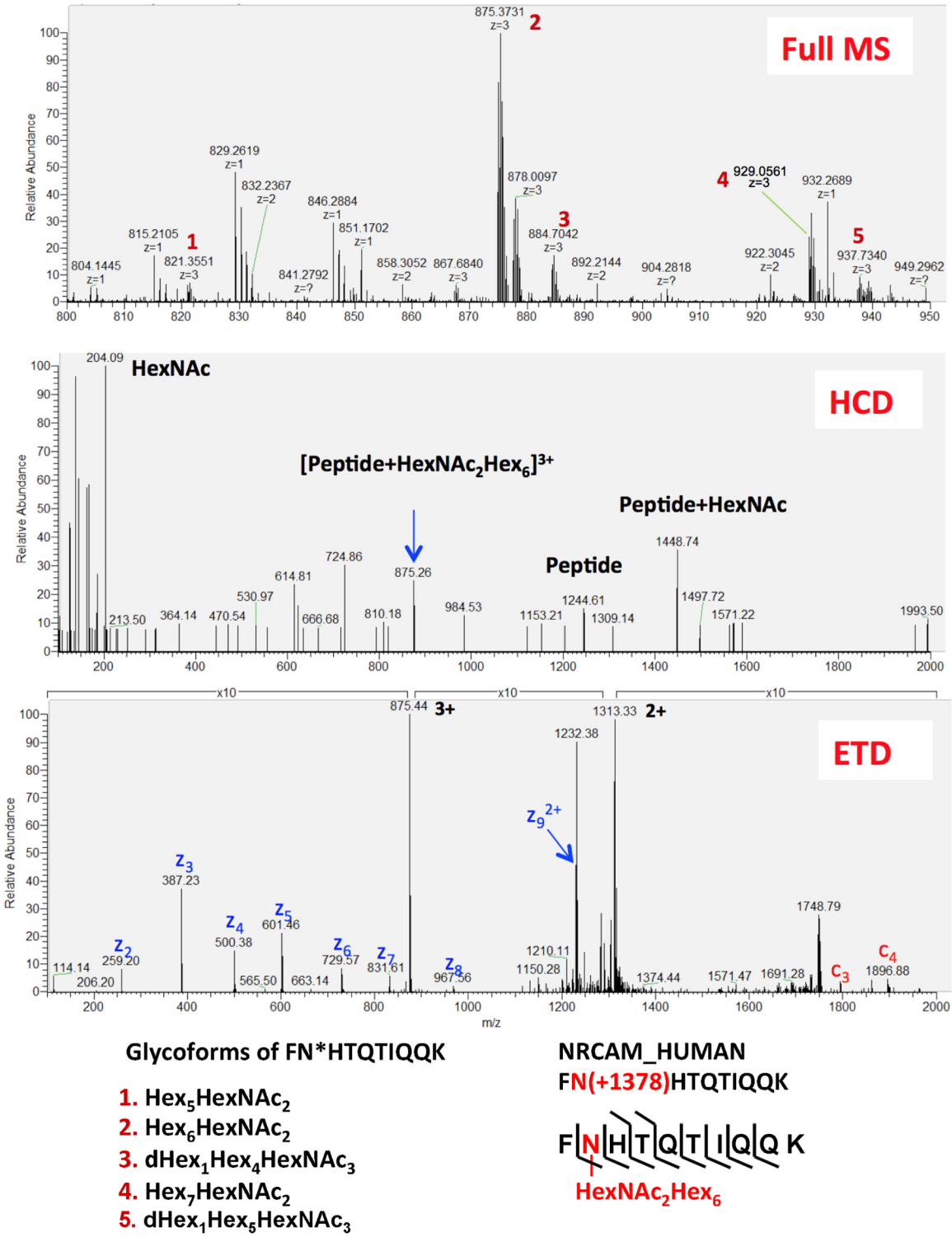

FIG. 3. **HCD-pd-ETD fragmentation.** Full MS showing the different glycoforms of the same peptide sequence *(A)*. Characteristic oxonium ion detected by HCD at m/z = 204.09 *(B)*. This HexNAc signature triggered an ETD scan to identify the peptide sequence and confirm the glycosylation site *(C)*.

ture, sugars tend to be arranged in branched polymers, resulting in an exponential increase of possible polysaccharide combinations. Theoretically, just six monosaccharides can give rise to 10^{12} different glycan structures. This high diversity of protein-bound glycans requires a combination of different techniques. For example, new MS-based methods were de-

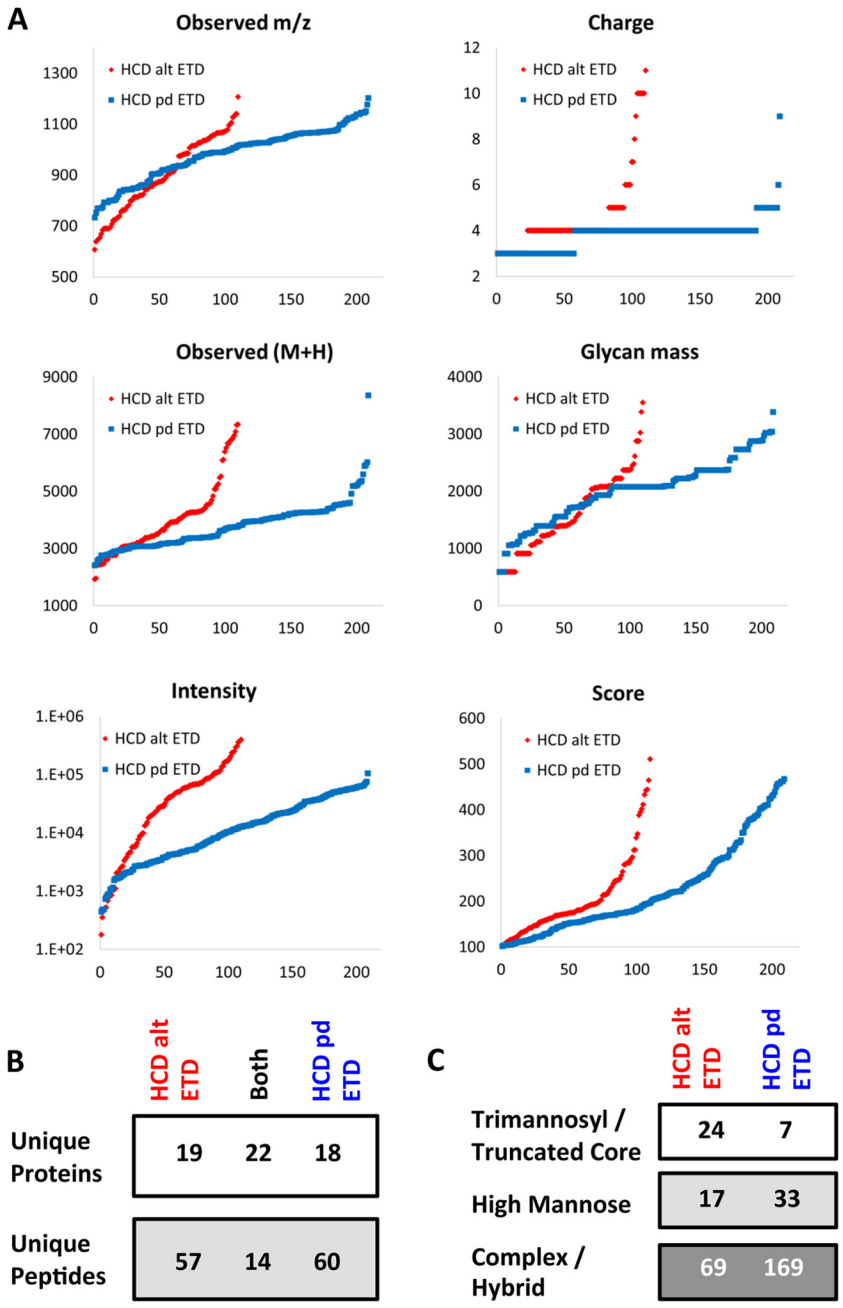

FIG. 4. **Comparison of HCD-pd-ETD and HCD-alt-ETD.** The two methods, HCD-pd-ETD (blue) and HCD-alt-ETD (red), displayed distinct distributions of the observed *m/z*, charge state, mass of identified peptides (M+H), and glycan mass, as well as the intensity of the precursor ions and the Byonics™ score (all *y*-axes). The *x*-axes represent index numbers after proteins were sorted by their corresponding *y*-axis value from lower to higher (*A*). There was limited overlap in the identified glycopeptides (*B*). *C*, the HCD-pd-ETD method preferentially identified complex/hybrid glycans.

veloped to profile the cell surface N-glycoproteome as a differentiation marker for stem cells (32). We applied a combination of different glycoproteomics techniques to further enrich for secreted and shed membrane proteins and reveal potential glycosylation sites within the endothelial secretome. Glycoproteins play important roles in many biological processes related to ECs, such as angiogenesis, in which the structural change of the glycans will determine the attachment property of cells and influence cell-to-cell interactions (33). Interestingly, vWF is a glycoprotein produced uniquely by ECs and megakaryocytes. Previous publications investigating vWF isolated from plasma failed to identify glycosylation sites within the propeptide (29). In plasma, the concentration of the propeptide is about one-tenth of the concentration of mature vWF (34, 35). In the conditioned medium of ECs, however, we observed several glycopeptides of the propeptide. Thus, the

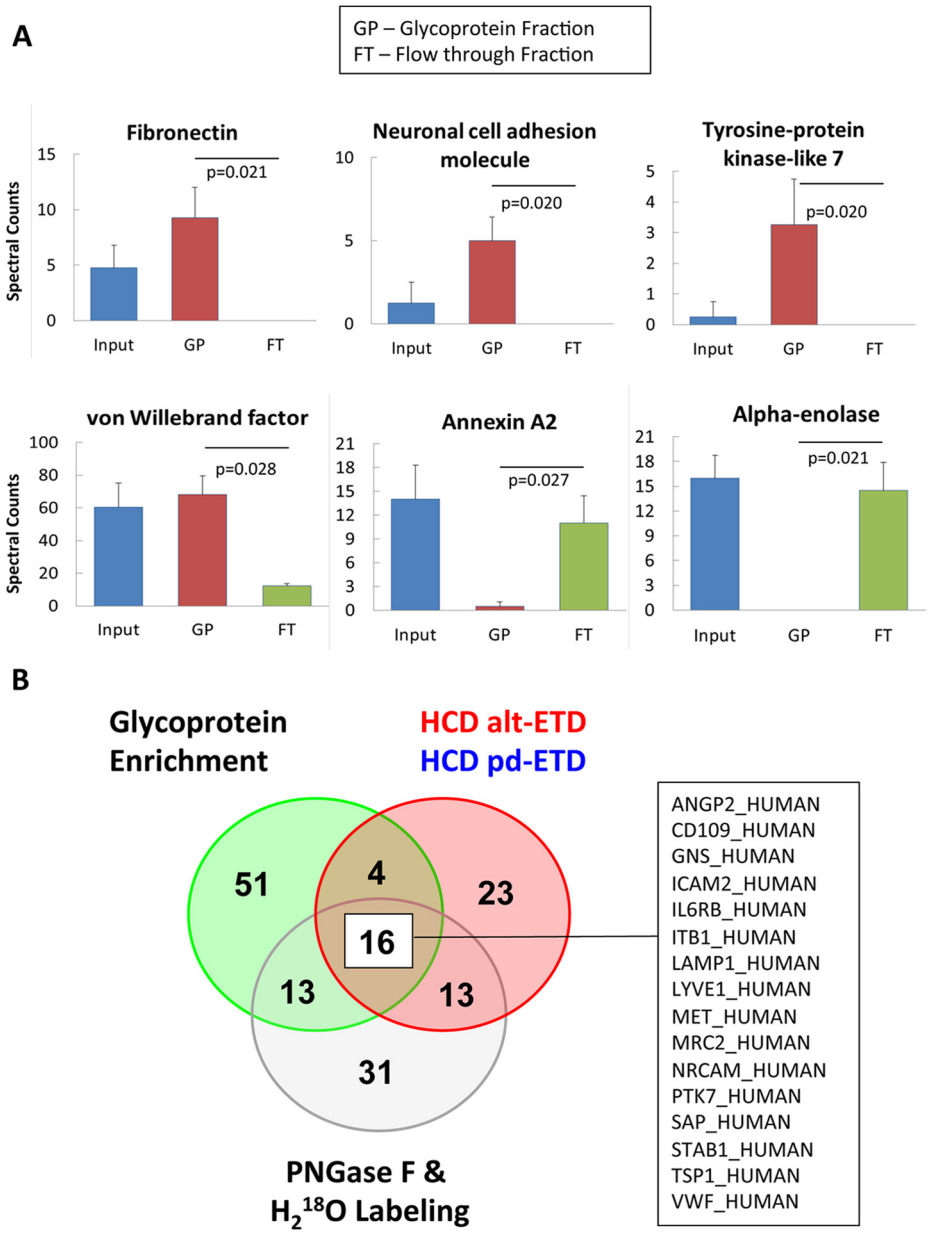

FIG. 5. **Glycoprotein enrichment for validation.** *A*, spectral count of input, glycoprotein-enriched fraction (GP), and flow-through fraction (FT) from representative glycoproteins and non-glycoproteins. *B*, complementarity of the different methods (HCD-ETD, PNGase F + $H_2{}^{18}O$ treatment, and glycoprotein enrichment). Only 18 glycoproteins were consistently identified.

endothelial secretome allowed us to interrogate the glycosylation sites of von Willebrand antigen 2, the N-terminal cleavage product of vWF that aids N-terminal multimerization and protein compartmentalization of mature vWF in storage granules.

Conventional Methods for Glycoproteomics—As reviewed elsewhere (36), conventional glycoproteomic methods involve the enrichment of glycoproteins (typically with lectins like ConA and wheat germ agglutinin), cleavage of the glycans, and identification of the remaining peptide sequence. The most widely used method for detecting N-glycopeptides is digestion by PNGase F. PNGase F cleaves the GlcNAc molecule closest to the peptide (37). After PNGase F treatment, formerly *N*-linked glycosylated peptides are identified based on the conversion of Asn to Asp (deamidation) in the consensus motif for *N*-linked glycosylation (sequence N-X(not P)-S/T). This method has two major caveats. The first of these is a high false positive rate due to spontaneous deamidation. Asn-Gly sites, in particular, are prone to spontaneous deamidation (38–40). To reduce false positives, PNGase F treatment is performed in ^{18}O water, adding a larger tag of 2.99 Da. Importantly, all known glycosyltransferases that mediate *N*-linked glycosylation are supposed to recognize a consensus motif, and this consensus sequence for *N*-linked glycosylation

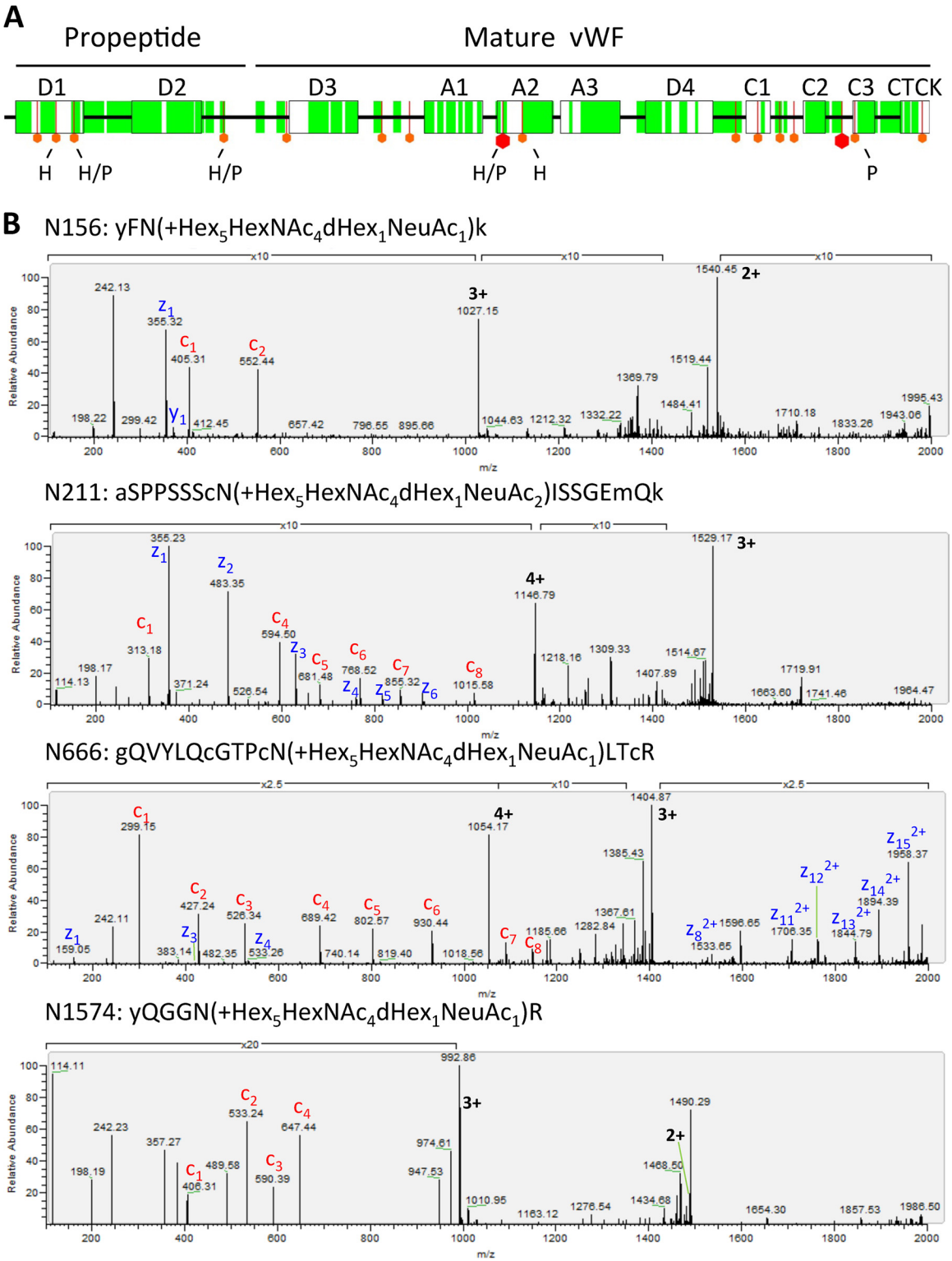

FIG. 6. **Sequence coverage for vWF.** *A*, schematic illustration of vWF sequence. Coverage is highlighted in green, and potential glycosylation sites are shown in red. A large hexagon indicates a glycosylation site with a reference in the Uniprot database. By using the HCD-ETD (H) or PNGase F (P) method, we confirmed six N-glycosylation sites on vWF. *B*, ETD spectra of glycopeptides identified via HCD-ETD (N156, N211, N666, N1574). The following abbreviations are used: a, y, g, k = TMT modified Ala, Tyr, Gly, and Lys, respectively; c = carboxyamidomethylation of Cys; m = oxidation of Met.

must be taken into consideration (41). 2) The second caveat is that after PNGase F cleavage, the released sugars can be analyzed separately, but the link to the identified peptides with deamidated amino acids is lost (42, 43). Ideally, intact glycopeptides are analyzed directly via MS/MS even in complex biological samples.

Novel HCD-ETD Method—HCD fragmentation mostly breaks glycosidic bonds, whereas ETD preserves the glycan attachment and fragments the peptide backbone, providing more complete peptide sequence information. Current MS/MS acquisition strategies for glycopeptide analysis rely on the acquisition of MS/MS spectra for all precursor ions. In this study, HCD was employed to generate glycan oxonium ions and trigger an ETD spectrum in a data-dependent manner. HCD presents the sugar signatures within the low *m/z* range, which are otherwise lost as a result of the one-third rule of ion trap fragmentation (44). Glycopeptides with terminal HexNAc generate typically an *m/z* 204.0864 oxonium ion and its fragments at *m/z* 168.0653 and 138.0550. The oxonium ion and its fragments are measured with the high mass accuracy of the Orbitrap analyzer, and the unambiguous identification of the glycan oxonium ion generated by the HCD scan serves as a diagnostic marker for glycopeptides. This approach was compared against conventional HCD-alt-ETD scans using a complex biological sample. The HCD-alt-ETD preferentially detects higher charged and higher intensity precursor ions than HCD-pd-ETD. This might be because (i) a higher charge increases ETD fragmentation efficiency, resulting in more identified glycopeptides; (ii) high-charged precursors did not produce HCD spectra of sufficient quality to trigger ETD based on the diagnostic oxonium ions; or (iii) more abundant peptides were selected in HCD-alt-ETD because the instrument duty cycle is less efficient than in HCD-pd-ETD. Overall, the combination of multiple MS methods used in our study provides greater confidence in the identification of glycopeptides than studies relying on a single approach and offers complementary advantages in the assessment of the glycoproteome, notably, the simultaneous identification of the peptide sequence, the glycosylation site, and the glycan composition.

Study Limitations—*N*-linked and O-linked glycosylation are the two most common forms of glycosylation in mammals (45). Only *N*-linked glycosylation was analyzed in the present study. Unlike *N*-linked glycosylation, O-linked glycosylation has no consensus site (46). This makes the analysis of O-linked glycopeptides a more daunting task (47). Lectins are widely used for glycoprotein enrichment. There are many types of lectins binding to different sugars, such as ConA (binds to α-D-mannosyl and α-D-glucosyl residues) and wheat germ agglutinin (binds to GlcNAcβ1–4GlcNAcβ1–4GlcNAc- and N-acetylneuraminic acid). Here we used only ConA as a proof of principle to demonstrate the complementary results of multiple glycoprotein identification methods. ConA is known to display nonspecific avidity for hydrophobic ligands such as certain domains of tropomyosin (48). Furthermore, the standard protocol for the ConA glycoprotein enrichment kit is not optimized for cleanliness, and several known non-glycoproteins were also detected in the eluate samples. Sequential washes with low- and high-ionic-strength buffers before elution might have reduced this contamination (49). Also, mixing different lectins would increase the coverage of the glycoproteome in biological samples (39). Additional efforts are needed for a complete structural characterization of protein glycosylation; in particular, the quantitation of the occupancy rates and the identification of the glycan structure as complex/hybrid glycans cannot be discerned via our current MS approach.

CONCLUSIONS

Cardiovascular diseases arise from exposure to risk factors that induce complex pathophysiological perturbations of endothelial protein secretion. The recent advent of new proteomic technologies has enabled us to obtain information on the dynamic regulation of endothelial protein secretion. We present results from an extensive glycoproteomic analysis with information on glycan composition obtained via a direct MS method. Future proteomics studies linking endothelial secretory processes to cardiovascular risk factors and endothelial dysfunction will provide valuable insights about the mechanisms contributing to cardiovascular disease.

Acknowledgment—We thank Dr. Sarah Langley for assistance with the gene ontology annotation.

* This work was funded by the Department of Health via a National Institute for Health Research (NIHR) Biomedical Research Centre award to Guy's and St. Thomas' NHS Foundation Trust in partnership with King's College London and King's College Hospital NHS Foundation Trust. Dr. M. Mayr is supported by a Senior Research Fellowship of the British Heart Foundation.

S This article contains supplemental material.

** To whom correspondence should be addressed: Prof. Manuel Mayr, Cardiovascular Division, King's British Heart Foundation Centre, King's College London, 125 Coldharbour Lane, London SE5 9NU, UK, Tel.: +44 (0) 20 7848 5132, E-mail: manuel.mayr@kcl.ac.uk.

REFERENCES

1. Mayr, M., Mayr, U., Chung, Y. L., Yin, X., Griffiths, J. R., and Xu, Q. (2004) Vascular proteomics: linking proteomic and metabolomic changes. *Proteomics* **4,** 3751–3761
2. Pula, G., Perera, S., Prokopi, M., Sidibe, A., Boulanger, C. M., and Mayr, M. (2008) Proteomic analysis of secretory proteins and vesicles in vascular research. *Proteomics Clin. Appl.* **2,** 882–891
3. Pober, J. S., and Sessa, W. C. (2007) Evolving functions of endothelial cells in inflammation. *Nat. Rev. Immunol.* **7,** 803–815
4. Cai, H., and Harrison, D. G. (2000) Endothelial dysfunction in cardiovascular diseases: the role of oxidant stress. *Circ. Res.* **87,** 840–844
5. Libby, P., and Simon, D. I. (2001) Inflammation and thrombosis: the clot thickens. *Circulation* **103,** 1718–1720
6. Ross, R. (1999) Atherosclerosis—an inflammatory disease. *N. Engl. J. Med.* **340,** 115–126
7. Pellitteri-Hahn, M. C., Warren, M. C., Didier, D. N., Winkler, E. L., Mirza, S. P., Greene, A. S., and Olivier, M. (2006) Improved mass spectrometric proteomic profiling of the secretome of rat vascular endothelial cells. *J. Proteome Res.* **5,** 2861–2864

8. Tunica, D. G., Yin, X., Sidibe, A., Stegemann, C., Nissum, M., Zeng, L., Brunet, M., and Mayr, M. (2009) Proteomic analysis of the secretome of human umbilical vein endothelial cells using a combination of free-flow electrophoresis and nanoflow LC-MS/MS. *Proteomics* **9,** 4991–4996
9. Flora, J. W., Edmiston, J., Secrist, R., Li, G., Rana, G. S., Langston, T. B., and McKinney, W. (2008) Identification of in vitro differential cell secretions due to cigarette smoke condensate exposure using nanoflow capillary liquid chromatography and high-resolution mass spectrometry. *Anal. Bioanal. Chem.* **391,** 2845–2856
10. Burghoff, S., and Schrader, J. (2011) Secretome of human endothelial cells under shear stress. *J. Proteome Res.* **10,** 1160–1169
11. Hocking, S. L., Wu, L. E., Guilhaus, M., Chisholm, D. J., and James, D. E. (2010) Intrinsic depot-specific differences in the secretome of adipose tissue, preadipocytes, and adipose tissue-derived microvascular endothelial cells. *Diabetes* **59,** 3008–3016
12. Griffoni, C., Di Molfetta, S., Fantozzi, L., Zanetti, C., Pippia, P., Tomasi, V., and Spisni, E. (2011) Modification of proteins secreted by endothelial cells during modeled low gravity exposure. *J. Cell. Biochem.* **112,** 265–272
13. Brioschi, M., Lento, S., Tremoli, E., and Banfi, C. (2013) Proteomic analysis of endothelial cell secretome: a means of studying the pleiotropic effects of Hmg-CoA reductase inhibitors. *J. Proteomics* **78,** 346–361
14. Castagna, M., Takai, Y., Kaibuchi, K., Sano, K., Kikkawa, U., and Nishizuka, Y. (1982) Direct activation of calcium-activated, phospholipid-dependent protein kinase by tumor-promoting phorbol esters. *J. Biol. Chem.* **257,** 7847–7851
15. Jacobs, J. M., Waters, K. M., Kathmann, L. E., Camp, D. G., 2nd, Wiley, H. S., Smith, R. D., and Thrall, B. D. (2008) The mammary epithelial cell secretome and its regulation by signal transduction pathways. *J. Proteome Res.* **7,** 558–569
16. Zampetaki, A., Kiechl, S., Drozdov, I., Willeit, P., Mayr, U., Prokopi, M., Mayr, A., Weger, S., Oberhollenzer, F., Bonora, E., Shah, A., Willeit, J., and Mayr, M. (2010) Plasma microRNA profiling reveals loss of endothelial miR-126 and other microRNAs in type 2 diabetes. *Circ. Res.* **107,** 810–817
17. Margariti, A., Zampetaki, A., Xiao, Q., Zhou, B., Karamariti, E., Martin, D., Yin, X., Mayr, M., Li, H., Zhang, Z., De Falco, E., Hu, Y., Cockerill, G., Xu, Q., and Zeng, L. (2010) Histone deacetylase 7 controls endothelial cell growth through modulation of beta-catenin. *Circ. Res.* **106,** 1202–1211
18. Yin, X., Cuello, F., Mayr, U., Hao, Z., Hornshaw, M., Ehler, E., Avkiran, M., and Mayr, M. (2010) Proteomics analysis of the cardiac myofilament subproteome reveals dynamic alterations in phosphatase subunit distribution. *Mol. Cell. Proteomics* **9,** 497–509
19. Didangelos, A., Yin, X., Mandal, K., Baumert, M., Jahangiri, M., and Mayr, M. (2010) Proteomics characterization of extracellular space components in the human aorta. *Mol Cell. Proteomics* **9,** 2048–2062
20. Mayr, M., Grainger, D., Mayr, U., Leroyer, A. S., Leseche, G., Sidibe, A., Herbin, O., Yin, X., Gomes, A., Madhu, B., Griffiths, J. R., Xu, Q., Tedgui, A., and Boulanger, C. M. (2009) Proteomics, metabolomics, and immunomics on microparticles derived from human atherosclerotic plaques. *Circ. Cardiovasc. Genet.* **2,** 379–388
21. Pula, G., Mayr, U., Evans, C., Prokopi, M., Vara, D. S., Yin, X., Astroulakis, Z., Xiao, Q., Hill, J., Xu, Q., and Mayr, M. (2009) Proteomics identifies thymidine phosphorylase as a key regulator of the angiogenic potential of colony-forming units and endothelial progenitor cell cultures. *Circ. Res.* **104,** 32–40
22. Urbich, C., De Souza, A. I., Rossig, L., Yin, X., Xing, Q., Prokopi, M., Drozdov, I., Steiner, M., Breuss, J., Xu, Q., Dimmeler, S., and Mayr, M. (2011) Proteomic characterization of human early pro-angiogenic cells. *J. Mol. Cell. Cardiol.* **50,** 333–336
23. Hagglund, P., Bunkenborg, J., Elortza, F., Jensen, O. N., and Roepstorff, P. (2004) A new strategy for identification of N-glycosylated proteins and unambiguous assignment of their glycosylation sites using HILIC enrichment and partial deglycosylation. *J. Proteome Res.* **3,** 556–566
24. Saba, J., Dutta, S., Hemenway, E., and Viner, R. (2012) Increasing the productivity of glycopeptides analysis by using higher-energy collision dissociation-accurate mass-product-dependent electron transfer dissociation. *Int. J. Proteomics* **2012,** 560391
25. Bern, M., Cai, Y., and Goldberg, D. (2007) Lookup peaks: a hybrid of de novo sequencing and database search for protein identification by tandem mass spectrometry. *Anal Chem.* **79,** 1393–1400
26. Antonov, A. S., Lukashev, M. E., Romanov, Y. A., Tkachuk, V. A., Repin, V. S., and Smirnov, V. N. (1986) Morphological alterations in endothelial cells from human aorta and umbilical vein induced by forskolin and phorbol 12-myristate 13-acetate: a synergistic action of adenylate cyclase and protein kinase C activators. *Proc. Natl. Acad. Sci. U.S.A.* **83,** 9704–9708
27. Sadler, J. E. (1998) Biochemistry and genetics of von Willebrand factor. *Annu. Rev. Biochem.* **67,** 395–424
28. Matsui, T., Titani, K., and Mizuochi, T. (1992) Structures of the asparagine-linked oligosaccharide chains of human von Willebrand factor. Occurrence of blood group A, B, and H(O) structures. *J. Biol. Chem.* **267,** 8723–8731
29. Canis, K., McKinnon, T. A., Nowak, A., Haslam, S. M., Panico, M., Morris, H. R., Laffan, M. A., and Dell, A. (2012) Mapping the N-glycome of human von Willebrand factor. *Biochem. J.* **447,** 217–228
30. Simak, J., Holada, K., and Vostal, J. G. (2002) Release of annexin V-binding membrane microparticles from cultured human umbilical vein endothelial cells after treatment with camptothecin. *BMC Cell Biol.* **3,** 11
31. Hart, G. W., and Copeland, R. J. (2010) Glycomics hits the big time. *Cell* **143,** 672–676
32. Wollscheid, B., Bausch-Fluck, D., Henderson, C., O'Brien, R., Bibel, M., Schiess, R., Aebersold, R., and Watts, J. D. (2009) Mass-spectrometric identification and relative quantification of N-linked cell surface glycoproteins. *Nat. Biotechnol.* **27,** 378–386
33. Leth-Larsen, R., Lund, R. R., and Ditzel, H. J. (2010) Plasma membrane proteomics and its application in clinical cancer biomarker discovery. *Mol. Cell. Proteomics* **9,** 1369–1382
34. Madabhushi, S. R., Shang, C., Dayananda, K. M., Rittenhouse-Olson, K., Murphy, M., Ryan, T. E., Montgomery, R. R., and Neelamegham, S. (2012) von Willebrand factor (VWF) propeptide binding to VWF D'D3 domain attenuates platelet activation and adhesion. *Blood* **119,** 4769–4778
35. van Mourik, J. A., Boertjes, R., Huisveld, I. A., Fijnvandraat, K., Pajkrt, D., van Genderen, P. J., and Fijnheer, R. (1999) von Willebrand factor propeptide in vascular disorders: a tool to distinguish between acute and chronic endothelial cell perturbation. *Blood* **94,** 179–185
36. Pan, S., Chen, R., Aebersold, R., and Brentnall, T. A. (2011) Mass spectrometry based glycoproteomics—from a proteomics perspective. *Mol. Cell. Proteomics* **10,** R110.003251
37. Maley, F., Trimble, R. B., Tarentino, A. L., and Plummer, T. H., Jr. (1989) Characterization of glycoproteins and their associated oligosaccharides through the use of endoglycosidases. *Anal. Biochem.* **180,** 195–204
38. Flatmark, T. (1967) Multiple molecular forms of bovine heart cytochrome c. V. A comparative study of their physicochemical properties and their reactions in biological systems. *J. Biol. Chem.* **242,** 2454–2459
39. Zielinska, D. F., Gnad, F., Wisniewski, J. R., and Mann, M. (2010) Precision mapping of an in vivo N-glycoproteome reveals rigid topological and sequence constraints. *Cell* **141,** 897–907
40. Angel, P. M., Lim, J. M., Wells, L., Bergmann, C., and Orlando, R. (2007) A potential pitfall in 18O-based N-linked glycosylation site mapping. *Rapid Commun. Mass Spectrom.* **21,** 674–682
41. Palmisano, G., Melo-Braga, M. N., Engholm-Keller, K., Parker, B. L., and Larsen, M. R. (2012) Chemical deamidation: a common pitfall in large-scale N-linked glycoproteomic mass spectrometry-based analyses. *J. Proteome Res.* **11,** 1949–1957
42. Wuhrer, M., Deelder, A. M., and Hokke, C. H. (2005) Protein glycosylation analysis by liquid chromatography-mass spectrometry. *J. Chromatogr. B Analyt. Technol. Biomed. Life Sci.* **825,** 124–133
43. Morelle, W., and Michalski, J. C. (2007) Analysis of protein glycosylation by mass spectrometry. *Nat. Protoc.* **2,** 1585–1602
44. Zhang, M. Y., Pace, N., Kerns, E. H., Kleintop, T., Kagan, N., and Sakuma, T. (2005) Hybrid triple quadrupole-linear ion trap mass spectrometry in fragmentation mechanism studies: application to structure elucidation of buspirone and one of its metabolites. *J. Mass Spectrom.* **40,** 1017–1029
45. Tissot, B., North, S. J., Ceroni, A., Pang, P. C., Panico, M., Rosati, F., Capone, A., Haslam, S. M., Dell, A., and Morris, H. R. (2009) Glycoproteomics: past, present and future. *FEBS Lett.* **583,** 1728–1735
46. Hang, H. C., Yu, C., Kato, D. L., and Bertozzi, C. R. (2003) A metabolic labeling approach toward proteomic analysis of mucin-type O-linked glycosylation. *Proc. Natl. Acad. Sci. U.S.A.* **100,** 14846–14851

47. Zhao, P., Viner, R., Teo, C. F., Boons, G. J., Horn, D., and Wells, L. (2011) Combining high-energy C-trap dissociation and electron transfer dissociation for protein O-GlcNAc modification site assignment. *J. Proteome Res.* **10,** 4088–4104
48. Owen, J. B., Di Domenico, F., Sultana, R., Perluigi, M., Cini, C., Pierce, W. M., and Butterfield, D. A. (2009) Proteomics-determined differences in the concanavalin-A-fractionated proteome of hippocampus and inferior parietal lobule in subjects with Alzheimer's disease and mild cognitive impairment: implications for progression of AD. *J. Proteome Res.* **8,** 471–482
49. Ghosh, D., Krokhin, O., Antonovici, M., Ens, W., Standing, K. G., Beavis, R. C., and Wilkins, J. A. (2004) Lectin affinity as an approach to the proteomic analysis of membrane glycoproteins. *J. Proteome Res.* **3,** 841–850